

Supplemental File for:

Title: Cytochrome P450-Catalyzed Metabolism of Cannabidiol to the Active Metabolite
7-Hydroxy-Cannabidiol

Authors: Jessica L. Beers, Dong Fu, and Klarissa D. Jackson

CONTENTS

- I. **Supplemental Methods:** Incubations with time-dependent CYP-selective inhibitors.
- II. **Supplemental Tables and Figures:**
 - Supplemental Table S1.** Donor information for CYP2C19-genotyped human liver microsomes (HLM).
 - Supplemental Table S2.** Summary of CBD and CBD metabolites detected by LC-MS/MS.
 - Supplemental Figure S1.** Representative LC-MS/MS chromatogram and MS-MS product ion spectra and predicted fragmentation patterns of CBD and metabolite standards.
 - Supplemental Figure S2.** Representative LC-MS/MS chromatograms of CBD metabolites formed in HLM in the presence and absence of the metabolic cofactors NADPH and UDPGA.
 - Supplemental Figure S3.** Representative LC-MS/MS chromatograms of CBD metabolites formed in HLM in the presence and absence of CYP-selective chemical inhibitors.
 - Supplemental Figure S4.** 7-OH-CBD formation in the presence of time-dependent CYP-selective inhibitors.
 - Supplemental Figure S5.** Effect of CYP-selective chemical inhibitors on 7-OH-CBD metabolism.
 - Supplemental Figure S6.** Effect of CYP2C19, CYP2D6, and CYP3A inhibition on 7-OH-CBD depletion and 7-COOH-CBD formation.
 - Supplemental Figure S7.** Metabolism of 7-OH-CBD by recombinant CYP enzymes.
 - Supplemental Figure S8.** Representative LC-MS/MS chromatogram and MS-MS product ion spectra of CBD metabolites produced by recombinant CYP2C19.
 - Supplemental Figure S9.** Representative LC-MS/MS chromatogram and MS-MS product ion spectra of CBD metabolites produced by recombinant CYP3A4.
 - Supplemental Figure S10.** Deuterated cannabinoid metabolite formation by rCYP2C19, rCYP3A4, and HLM.
 - Supplemental Figure S11.** CYP2C19 activity, as measured by S-mephenytoin 4'-hydroxylation, in individual CYP2C19-genotyped HLM.
- III. **Reference**

Supplemental Methods: Incubations with time-dependent CYP-selective inhibitors.

CBD (1 μ M) was incubated in 150-donor pooled HLM (0.2 mg/mL protein) in the presence of the following time-dependent inhibitors: CYP3cide (0.5 μ M), furafylline (25 μ M), clomethiazole (30 μ M), ticlopidine (5 μ M), 4-methylpyrazole (100 μ M) or vehicle. Following a pre-incubation period with inhibitors and HLM, reactions were transferred to a secondary incubation containing substrate for 10 min. The preincubation period was 30 min for reactions containing clomethiazole and 10 min for all other inhibitory conditions. For reactions containing the competitive CYP2E1 inhibitor 4-methylpyrazole, reactions were preincubated with buffer for 30 min prior to transfer to a secondary incubation containing both the substrate and 4-methylpyrazole. Metabolite formation was determined by LC-MS/MS analysis and was compared to incubations containing vehicle control to determine the percentage relative to control.

Supplier	Lot	CYP2C19 Genotype	Sex	Age	^a CYP2C19 Activity S-Mephenytoin 4'-Hydroxylation (pmol/min/mg)	^b CYP3A Activity Testosterone 6 β -Hydroxylation (pmol/min/mg)
XenoTech	710444	*1/*1	M	46	17.32	812
XenoTech	710450	*1/*1	M	60	81.3	7680
BioIVT	LLO	*1/*1	M	24	5.42	381
BioIVT	ONY	*1/*1	M	65	0.65	765
BioIVT	OED	*1/*1	M	75	4.38	269
BioIVT	IFF	*1/*1	M	53	2.50	477
BioIVT	QLC	*1/*1	M	48	3.30	1296
XenoTech	710456	*1/*2	M	21	49.86	2780
XenoTech	710415	*1/*2	F	62	5.25	1230
XenoTech	810010	*2/*2	M	49	1.81	572
Corning	HH689	*2/*2	M	69	2.03	2300
Corning	HH863	*2/*2	F	46	4.65	8700
Corning	HH40	*2/*2	M	66	3.28	2400
BioIVT	GWN	*1/*17	M	61	12.29	290
BioIVT	RYQ	*1/*17	M	31	3.24	185
BioIVT	TKM	*1/*17	M	56	23.27	293
BioIVT	YEJ	*17/*17	M	38	3.33	668
BioIVT	ZKI	*17/*17	M	59	34.56	813
BioIVT	ZGH	*17/*17	M	44	3.27	963

a. Donor CYP2C19 activity, as measured by rates of S-mephenytoin 4'-hydroxylation (pmol/min/mg protein), was determined as described previously (Murray et al., 2020). CYP2C19 activity data for lot 710450 was provided by XenoTech, LLC.

b. Donor CYP3A activity, as measured by rates of testosterone 6 β -hydroxylation (pmol/min/mg protein), values were provided by each vendor. Testosterone 6 β -hydroxylation rates for HLM lots from BioIVT are the rates determined at the K_m concentration for the probe substrate.

Supplemental Table S1. Donor information for CYP2C19-genotyped HLM. HLM from individual donors were purchased from Sekisui XenoTech, LLC. (Lenexa, KS), Corning Life Sciences (Woburn, MA), and BioIVT (Baltimore, MD). Samples were genotyped by the suppliers as follows: CYP2C19*1/*1 donors (n = 7), CYP2C19*1/*2 donors (n = 2), CYP2C19*2/*2 donors (n = 4), CYP2C19*1/*17 donors (n = 3), and CYP2C19*17/*17 donors (n = 3). Donors included 17 males (M) and two females (F); the median age was 51.2 years (range 21-75 years).

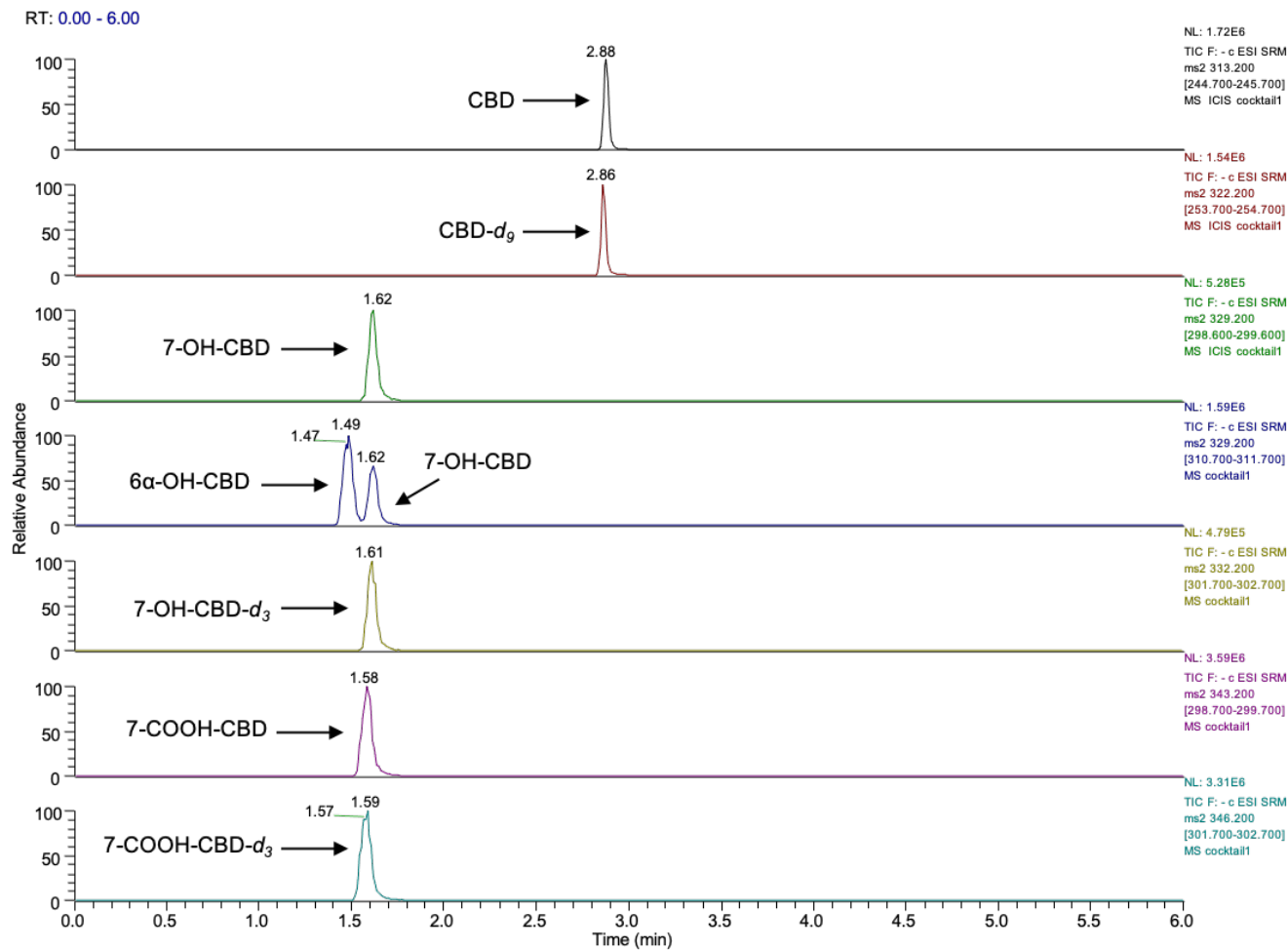
Analyte	^a m/z Transition	Retention Time (min)	LC Gradient Method	Major Enzyme System of Formation	Cofactor Dependence
CBD	313 > 245	2.88	3		
CBD-d ₉	322 > 254	2.86	3		
6 α -OH-CBD	329 > 311	1.49	3	HLM, 3A4	NADPH
^b 6 α -OH-CBD-d ₉	338 > 320	1.60	3	HLM, 3A4	NADPH
7-OH-CBD	329 > 299, 311	1.62	3	HLM, 2C9, 2C19	NADPH
7-OH-CBD-d ₃	332 > 302	1.61	3		
^b 7-OH-CBD-d ₉	338 > 308, 320	1.74	3	HLM, 2C19	NADPH
7-COOH-CBD	343 > 299	1.58	3	HLM, 2C19, 2D6	NADPH
^c 7-COOH-CBD-d ₃	346 > 302	1.59	3	HLM, 2C19	NADPH
CBD-glucuronide	489 > 313	1.32	3	HLM	UDPGA
M1	329 > 311	1.71	3	HLM, 3A4	NADPH
M2	329 > 299	1.99	3	HLM, 3A4	NADPH
M3	343 > 299	2.15	3	HLM, 2C19, 3A4	NADPH
M4	343 > 299	1.79	3	2C19	NADPH
M5	329 > 311	2.36	3	3A4	NADPH

a. Multiple reaction monitoring in negative ion mode (ESI⁻).

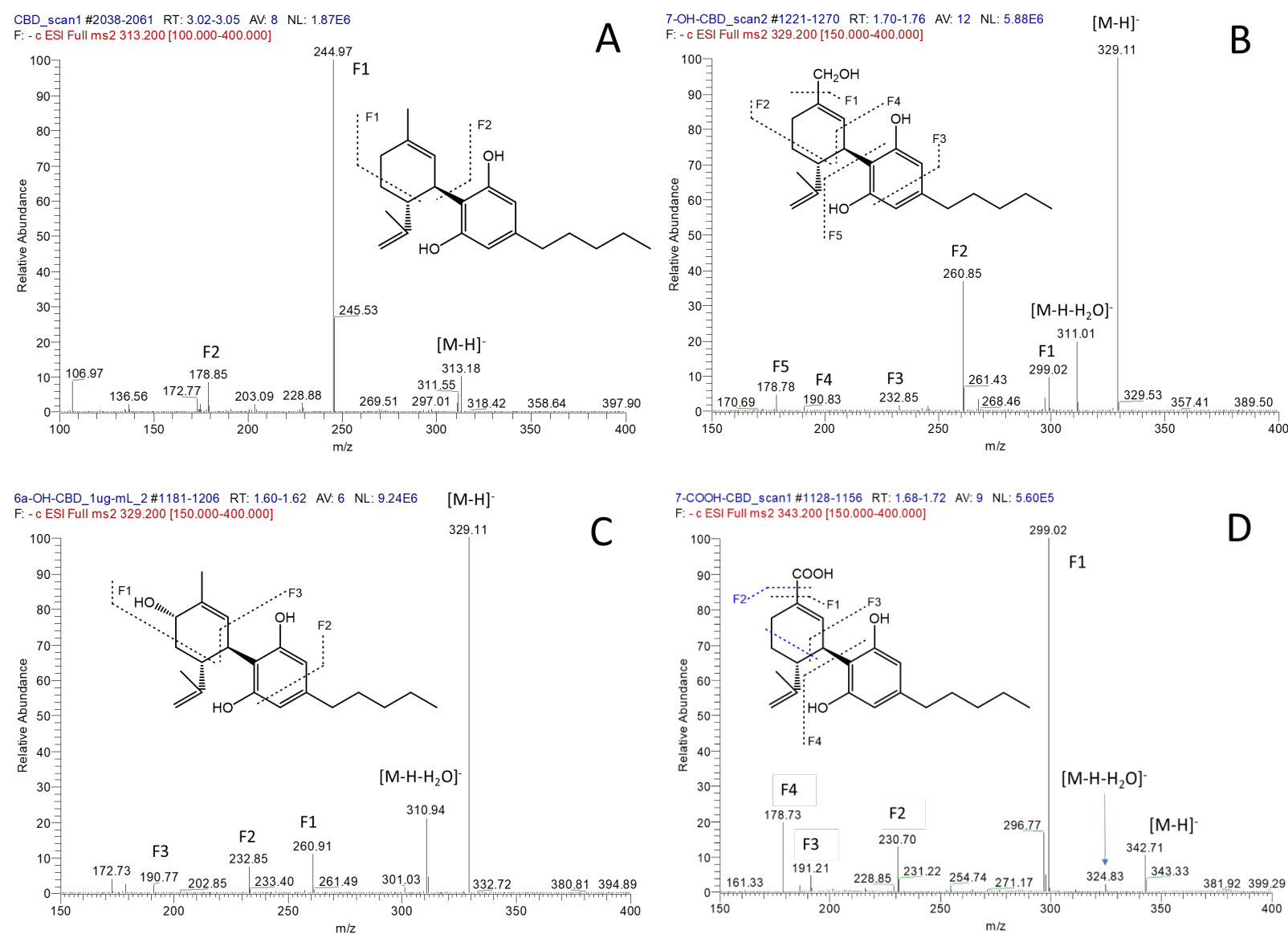
b. Indicates 6 α -OH-CBD-d₉ and 7-OH-CBD-d₉ formation when CBD-d₉ was used as a substrate

c. Indicates 7-COOH-CBD-d₃ formation when 7-OH-CBD-d₃ was used as a substrate

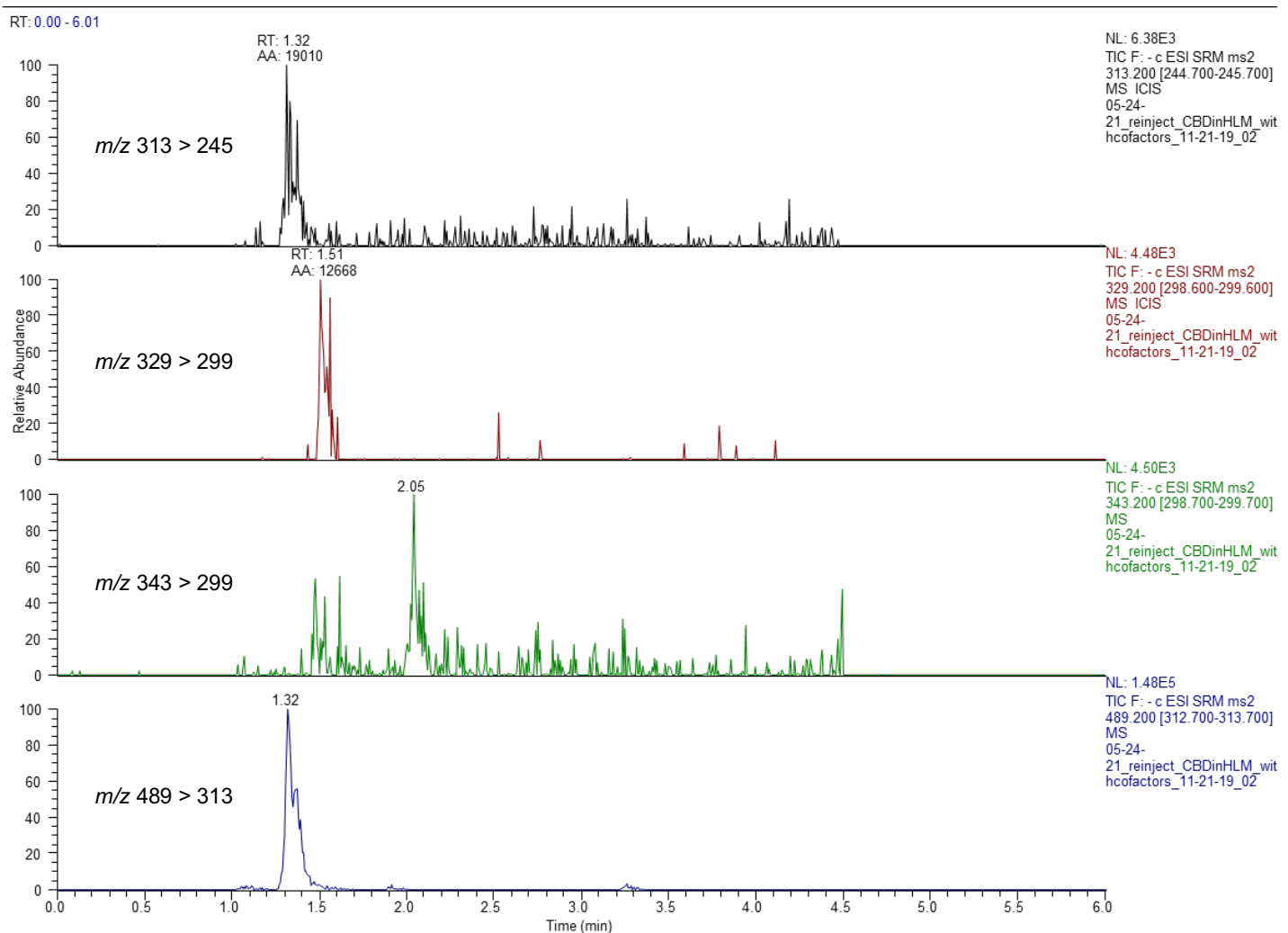
Supplemental Table S2. Summary of CBD and CBD metabolites detected by LC-MS/MS



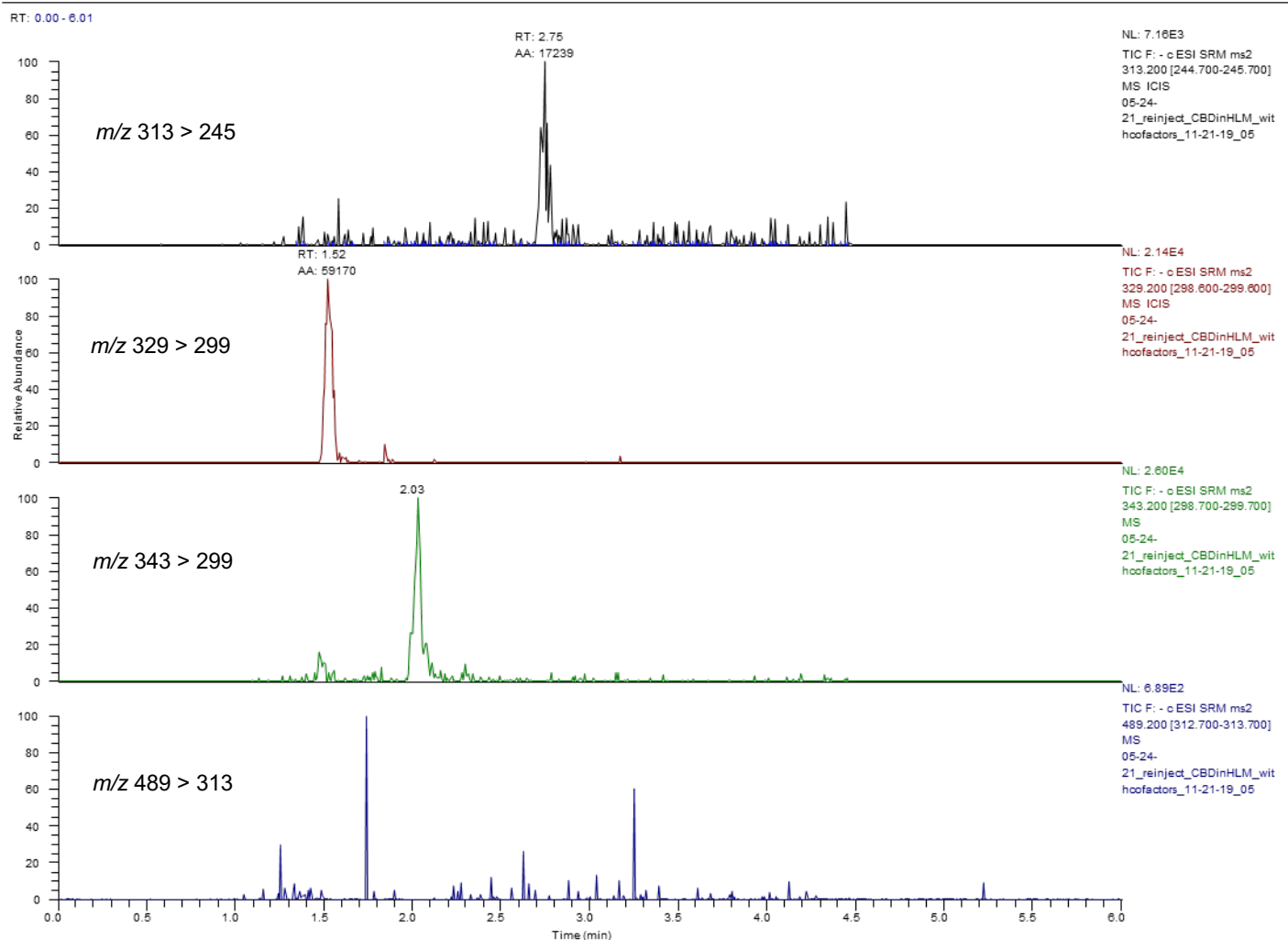
Supplemental Figure S1A. Representative LC-MS/MS chromatogram of CBD, metabolite standards, and internal standards (1 µg/ml). Selected reaction monitoring in the negative ion mode [M - H]⁻ was used for detecting CBD and its metabolites with the following precursor-to-product ion transitions: CBD (*m/z* 313 > 245), CBD-d₉ (internal standard) (*m/z* 322 > 254), 7-OH-CBD (*m/z* 329 > 299 and 329 > 311), 6α-OH-CBD (*m/z* 329 > 311), 7-OH-CBD-d₃ (*m/z* 332 > 302), 7-COOH-CBD (*m/z* 343 > 299) and 7-COOH-CBD-d₃ (*m/z* 346 > 302). The total ion chromatogram (TIC) is shown (top) for all MRM transitions monitored.



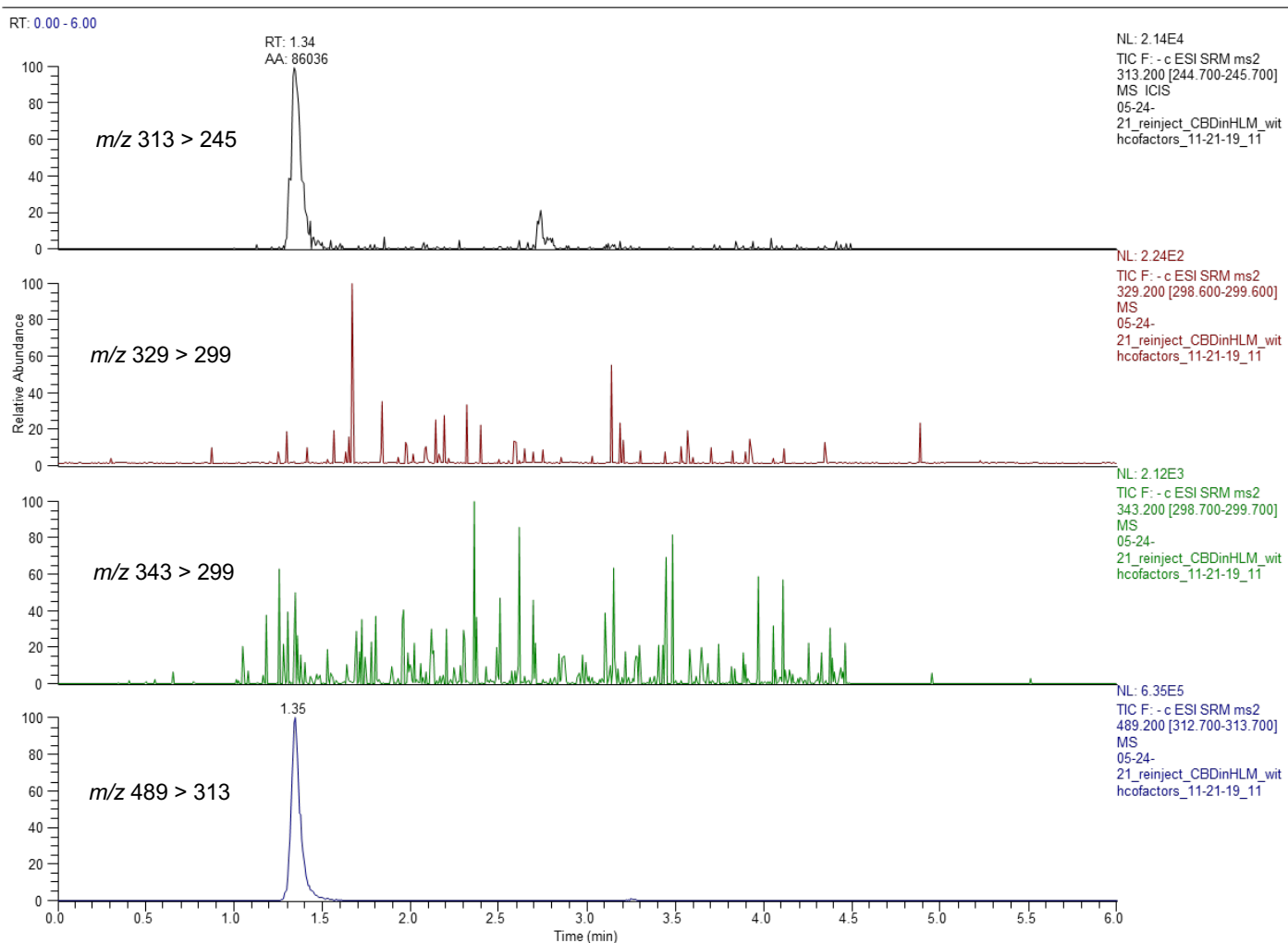
Supplemental Figure S1B. Representative product ion spectra and predicted fragmentation patterns from LC-MS/MS analysis of 1 μ g/mL CBD and metabolite standards. Product scans were conducted in the negative ion mode $[M - H]^-$ with the following precursor ions: CBD (m/z 313) (A), 7-hydroxy-CBD (m/z 329) (B), 6 α -hydroxy-CBD (m/z 329) (C), and 7-carboxy-CBD (m/z 343) (D). The predicted sites of fragmentation for each compound are shown.



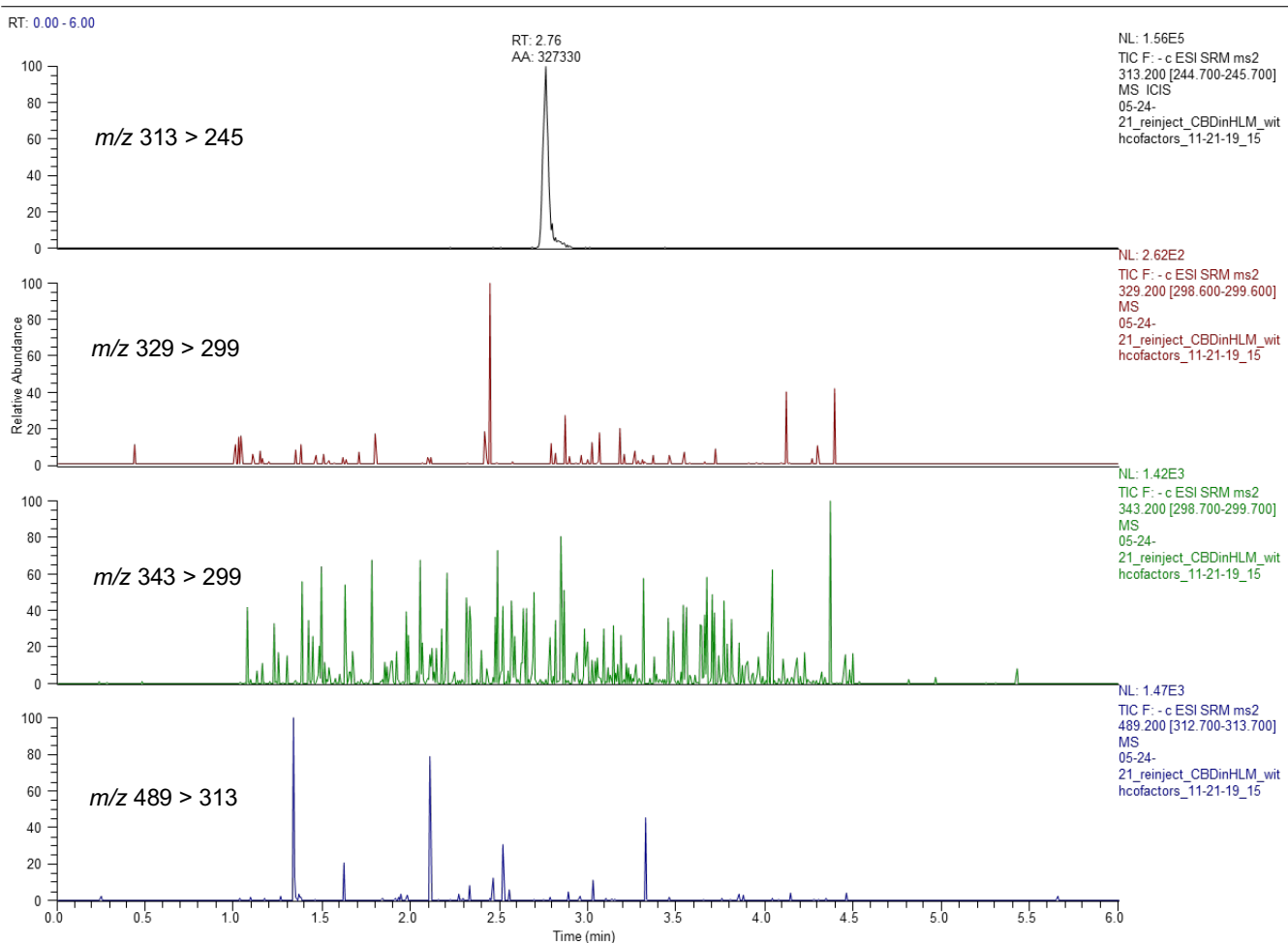
Supplemental Figure S2A. Representative LC-MS/MS chromatograms of CBD metabolites formed in HLM in the presence of NADPH and UDPGA. CBD (1 μ M) was incubated with 150-donor pooled HLM for 60 min. Metabolites were identified by LC-MS/MS using the following precursor-to-product ion transitions (top to bottom): likely the CBD-glucuronide (retention time 1.32 min, m/z 313 > 245, due to in-source fragmentation), 7-OH-CBD (retention time 1.51 min, m/z 329 > 299), M3 (retention time 2.05 min, m/z 343 > 299), and CBD-glucuronide (retention time 1.32 min, m/z 489 > 313).



Supplemental Figure S2B. Representative LC-MS/MS chromatograms of CBD metabolites formed in HLM in the presence of NADPH only. CBD (1 μ M) was incubated with 150-donor pooled HLM for 60 min with NADPH and without UDPGA. Metabolites were identified by LC-MS/MS using the following precursor-to-product ion transitions (top to bottom): CBD (retention time 2.75 min, m/z 313 > 245), 7-OH-CBD (retention time 1.52 min, m/z 329 > 299), M3 (retention time 2.03 min, m/z 343 > 299), and CBD-glucuronide (not detected, m/z 489 > 313).

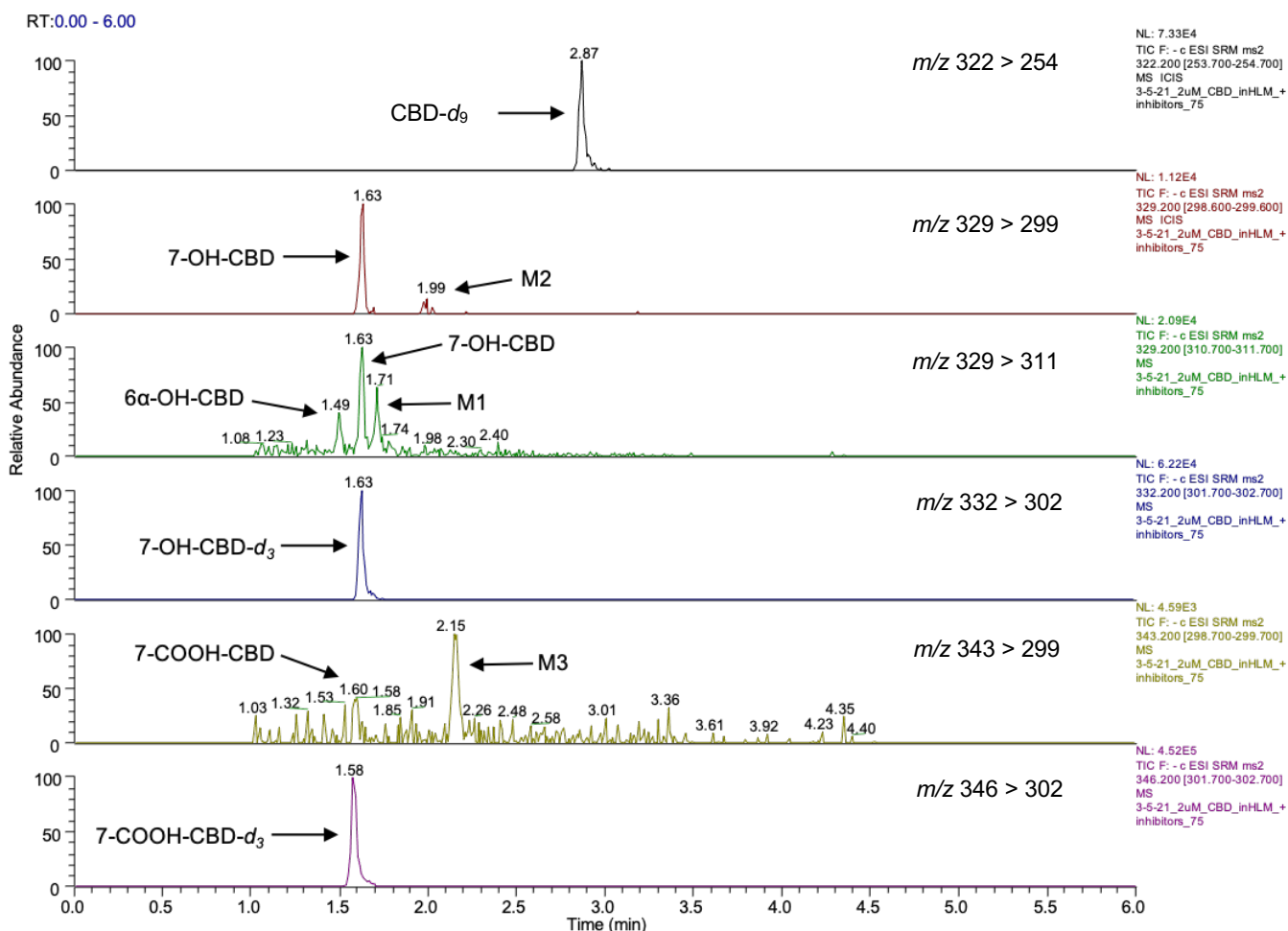


Supplemental Figure S2C. Representative LC-MS/MS chromatograms of CBD metabolites formed in HLM in the presence of UDPGA only. CBD (1 μ M) was incubated with 150-donor pooled HLM for 60 min with UDPGA and without NADPH. Metabolites were identified by LC-MS/MS using the following precursor-to-product ion transitions (top to bottom): likely the CBD-glucuronide (retention time 1.34 min, $m/z\ 313 > 245$, due to in-source fragmentation), 7-OH-CBD (not detected, $m/z\ 329 > 299$), 7-COOH-CBD (not detected, $m/z\ 343 > 299$), and CBD-glucuronide (retention time 1.35 min, $m/z\ 489 > 313$).



Supplemental Figure S2D. Representative LC-MS/MS chromatograms of CBD metabolites formed in HLM in the absence of cofactors. CBD (1 μ M) was incubated with 150-donor pooled HLM for 60 min without NADPH or UDPGA. Metabolites were identified by LC-MS/MS using the following precursor-to-product ion transitions (top to bottom): CBD (retention time 2.76 min, $m/z\ 313 > 245$), 7-OH-CBD (not detected, $m/z\ 329 > 299$), 7-COOH-CBD (not detected, $m/z\ 343 > 299$), CBD-glucuronide (not detected, $m/z\ 489 > 313$).

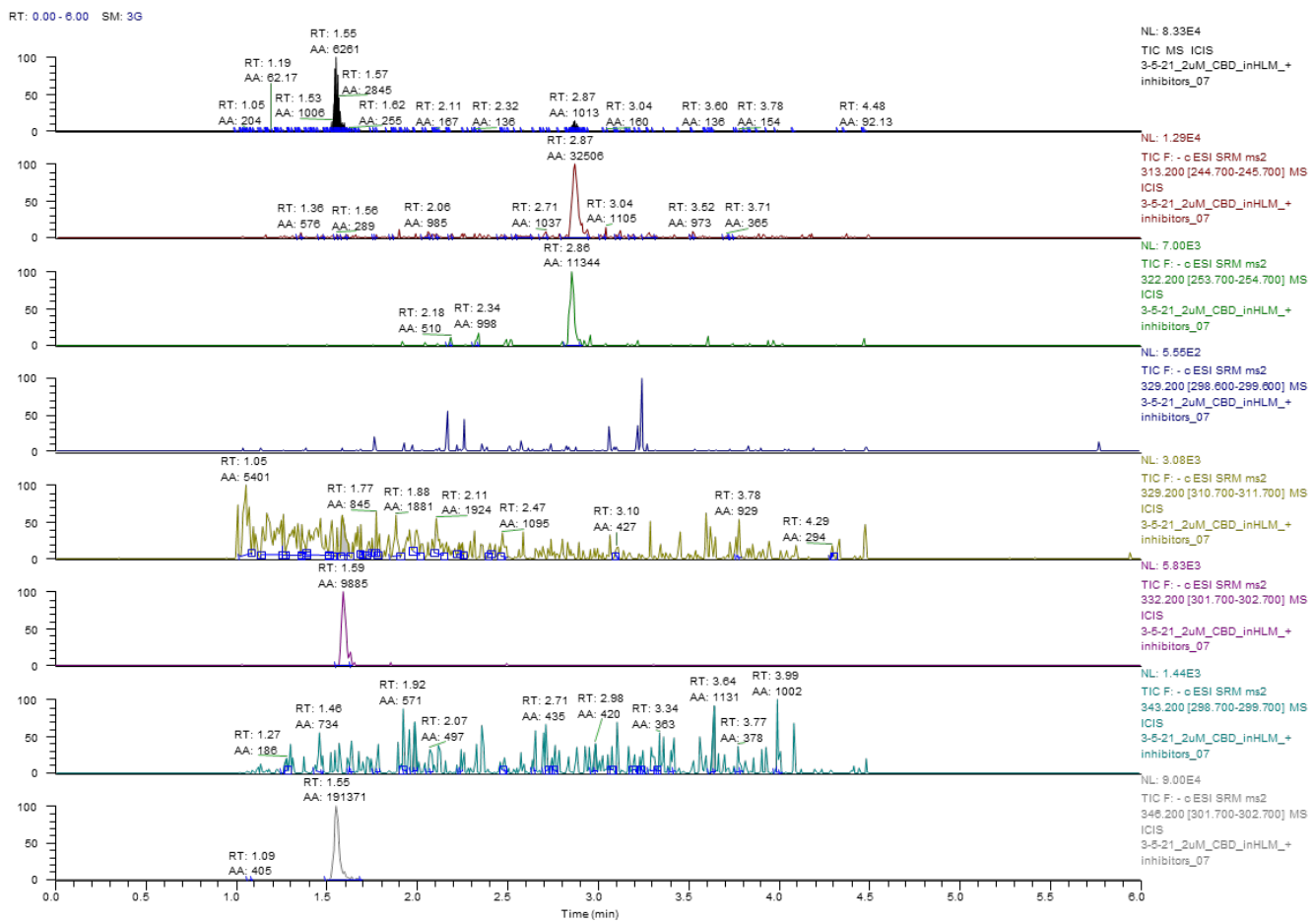
Supplemental Figure S3. CBD metabolism in the presence of CYP-selective chemical inhibitors. CBD (2 μ M) was incubated with pooled HLM (0.2 mg/mL protein) for 10 min with NADPH in the presence of the following CYP-selective inhibitors: vehicle control (+NADPH) (A), vehicle control (-NADPH) (B), 1 μ M α -naphthoflavone (CYP1A2 inhibitor) (C), 25 μ M furafylline (CYP1A2 inhibitor) (D), 15 μ M PPP (CYP2B6 inhibitor) (E), 5 μ M ticlopidine (CYP2C19 and CYP2B6 inhibitor) (F), 5 μ M sulfaphenazole (CYP2C9 inhibitor) (G), 5 μ M (+)-*N*-3-benzyl nirvanol (CYP2C19 inhibitor) (H), 2 μ M quinidine (CYP2D6 inhibitor) (I), 100 μ M 4-methylpyrazole (CYP2E1 inhibitor) (J), or 1 μ M ketoconazole (CYP3A4 and CYP3A5 inhibitor) (K). Metabolite formation was measured by LC-MS/MS.



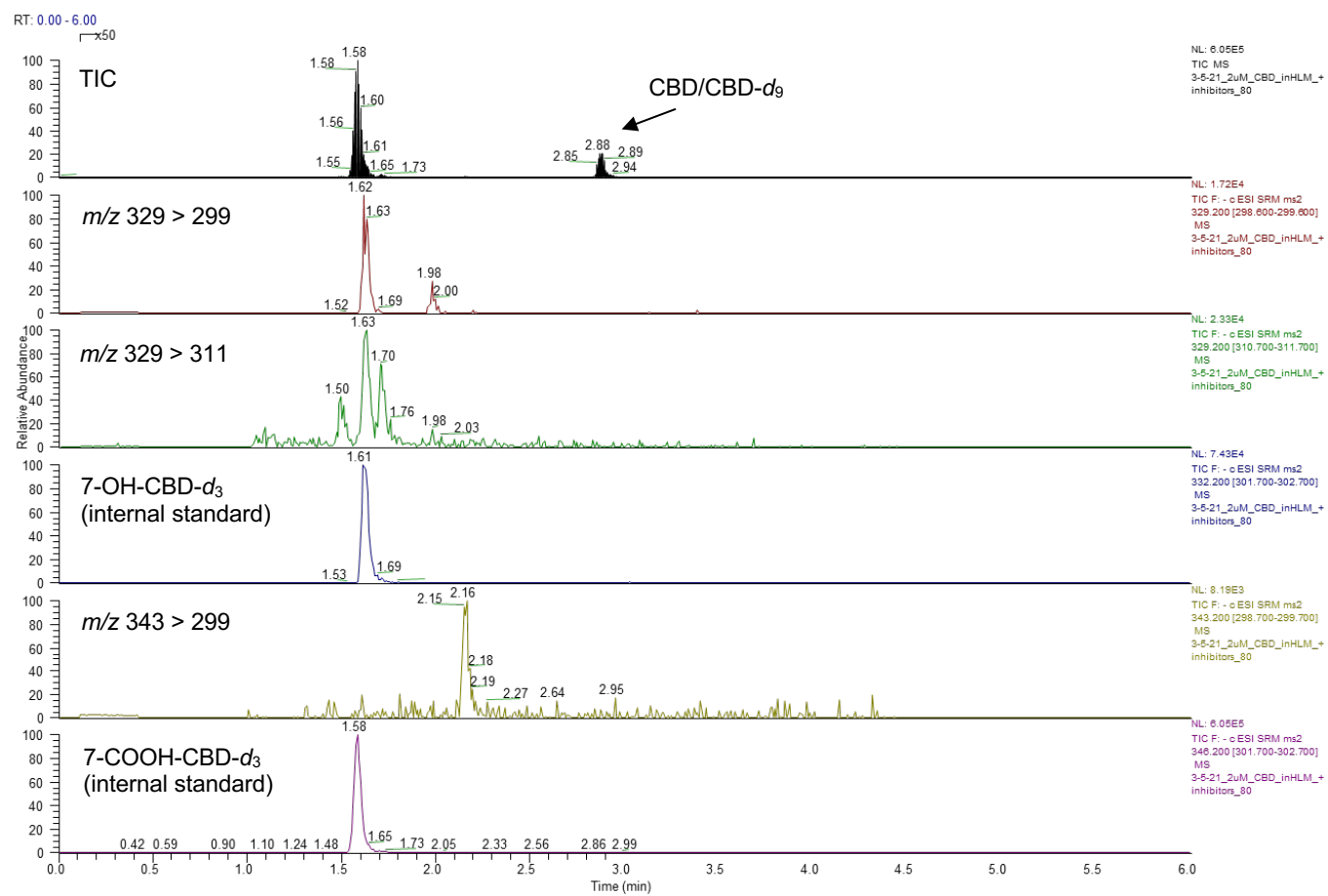
Supplemental Figure S3A. CBD (2 μ M) metabolism in HLM, vehicle control (+NADPH). Mass transitions are as follows: CBD- d_9 (2.87 min, m/z 322 > 254), 7-OH-CBD (1.63 min, m/z 329 > 299 and 329 > 311), M2 (1.99 min, m/z 329 > 299), 6 α -OH-CBD (1.49 min, m/z 329 > 311), M1 (1.71 min, m/z

DMD-AR-2020-000350R2

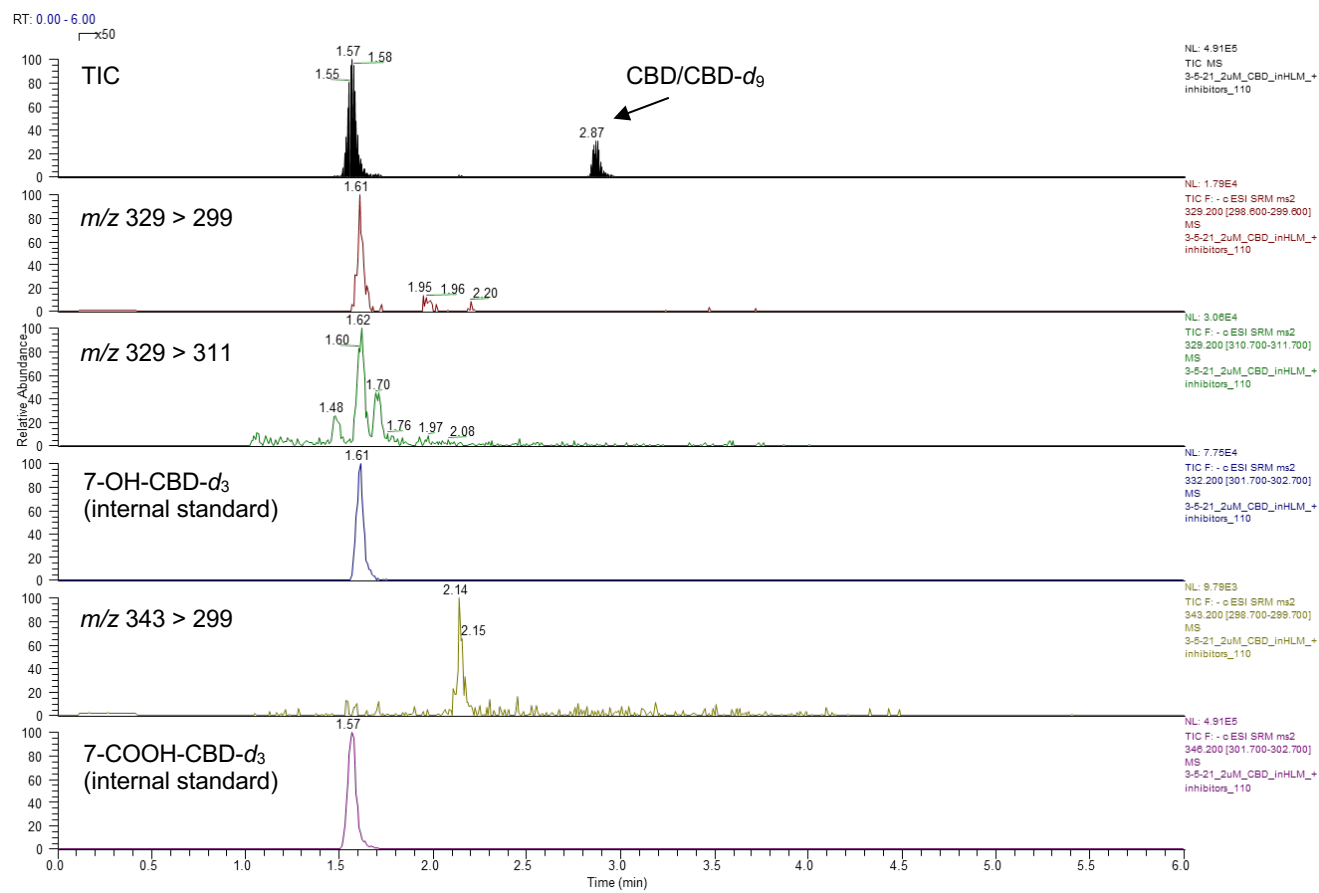
329 > 311), 7-OH-CBD- d_3 (1.63 min, m/z 332 > 302), 7-COOH-CBD (1.6 min, m/z 343 > 299), M3 (2.15 min, m/z 343 > 299), and 7-COOH-CBD- d_3 (m/z 346 > 302).



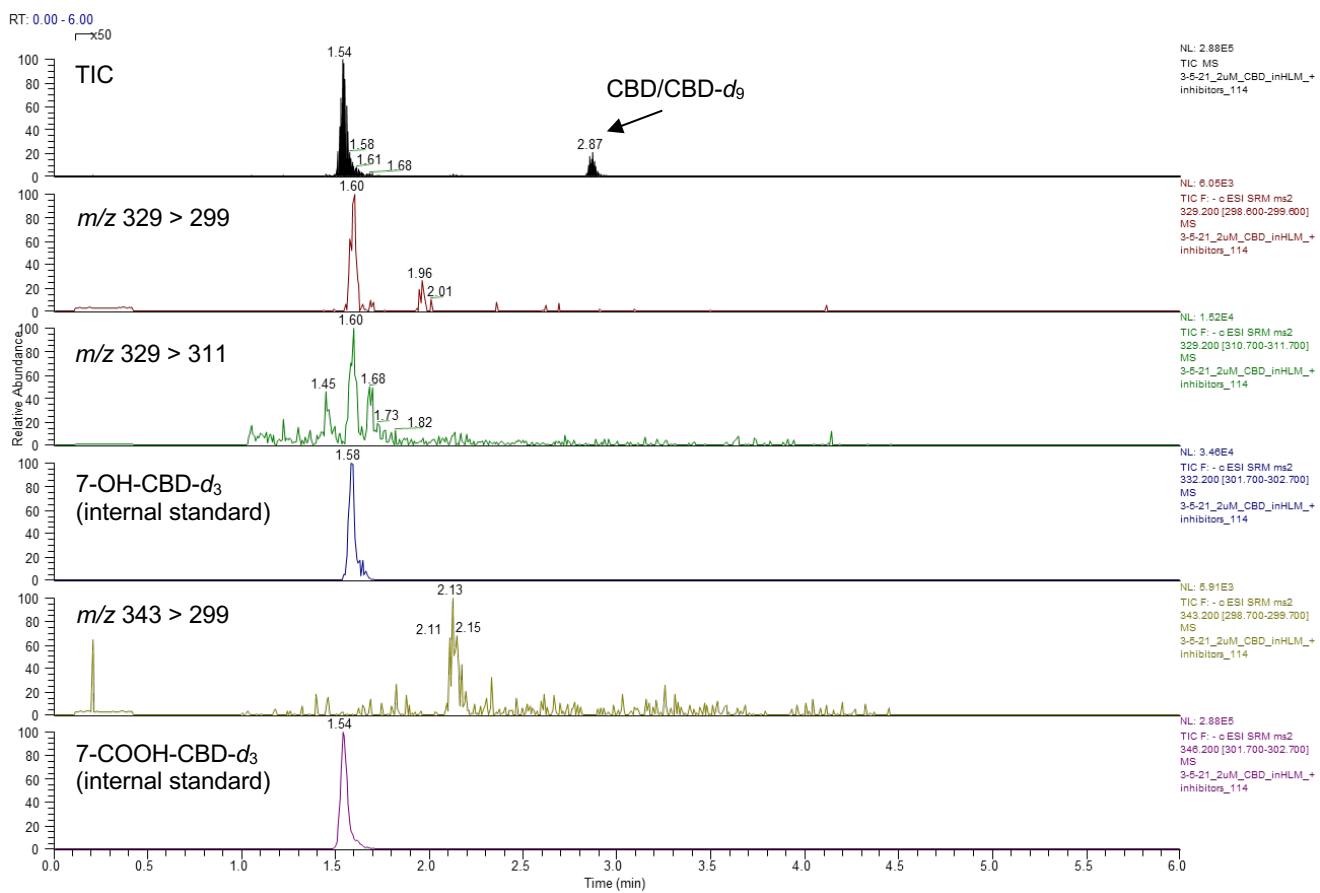
Supplemental Figure S3B. CBD (2 μ M) metabolism in HLM, vehicle control (-NADPH). The total ion chromatogram (TIC) is shown (top) for all MRM transitions monitored. Mass transitions are as follows: CBD (2.87 min, m/z 313 > 245), CBD-d₉ (2.86 min, 322 > 254), 7-OH-CBD (not detected, m/z 329 > 299 and 329 > 311), 7-OH-CBD-d₃ (1.59 min, m/z 332 > 302), 7-COOH-CBD (not detected, m/z 343 > 299), and 7-COOH-CBD-d₃ (m/z 346 > 302).



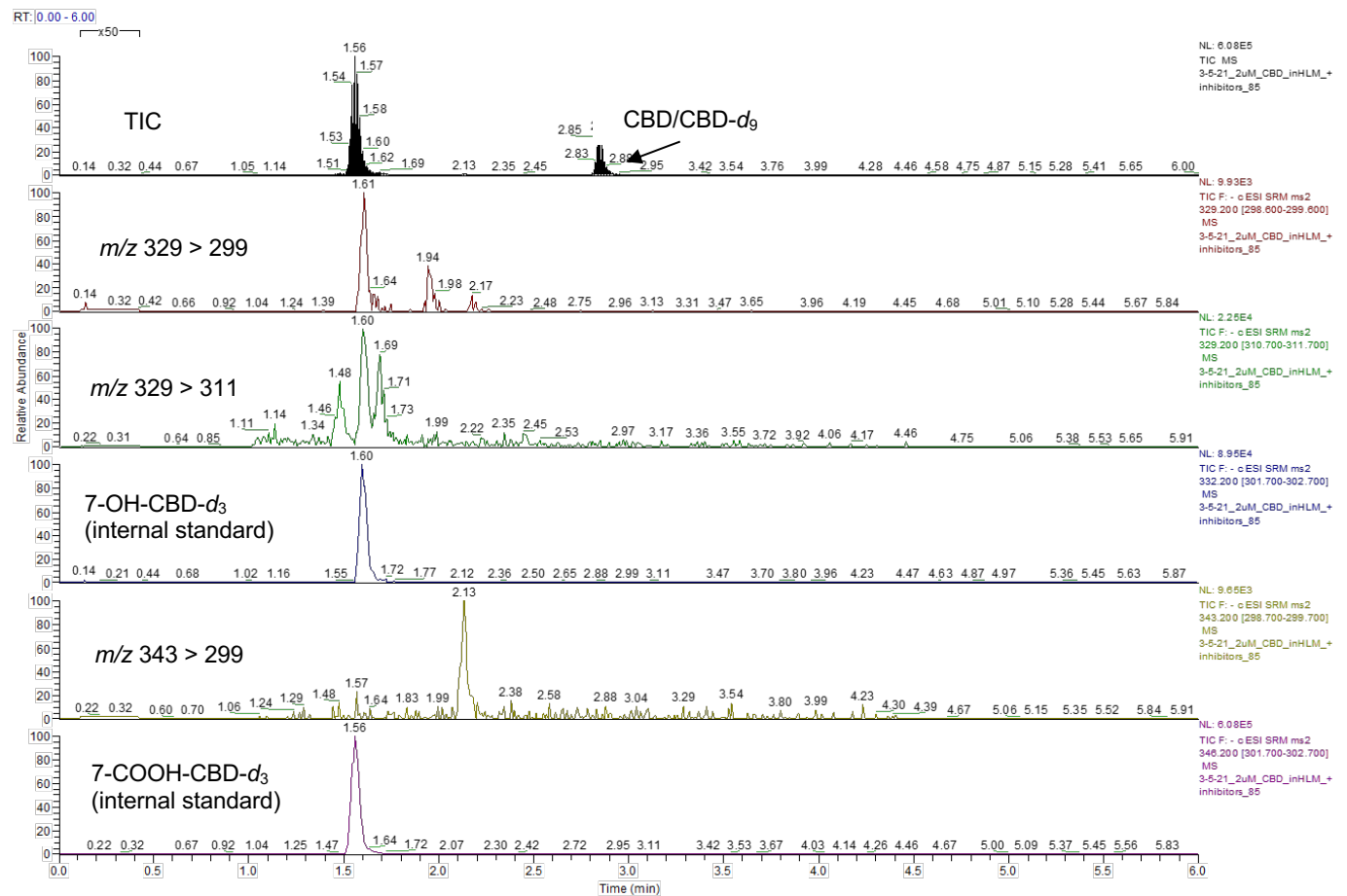
Supplemental Figure S3C. CBD (2 μ M) metabolism in HLM in the presence of α -naphthoflavone. The total ion chromatogram (TIC) is shown (top) for all MRM transitions monitored. Mass transitions are as follows: 7-OH-CBD (1.62 min, m/z 329 > 299 and 329 > 311), M2 (1.98 min, m/z 329 > 299), 6 α -OH-CBD (1.5 min, m/z 329 > 311), M1 (1.7 min, m/z 329 > 311), 7-OH-CBD-d₃ (1.61 min, m/z 332 > 302), M3 (2.16 min, m/z 343 > 299), and 7-COOH-CBD-d₃ (1.58 min, m/z 346 > 302).



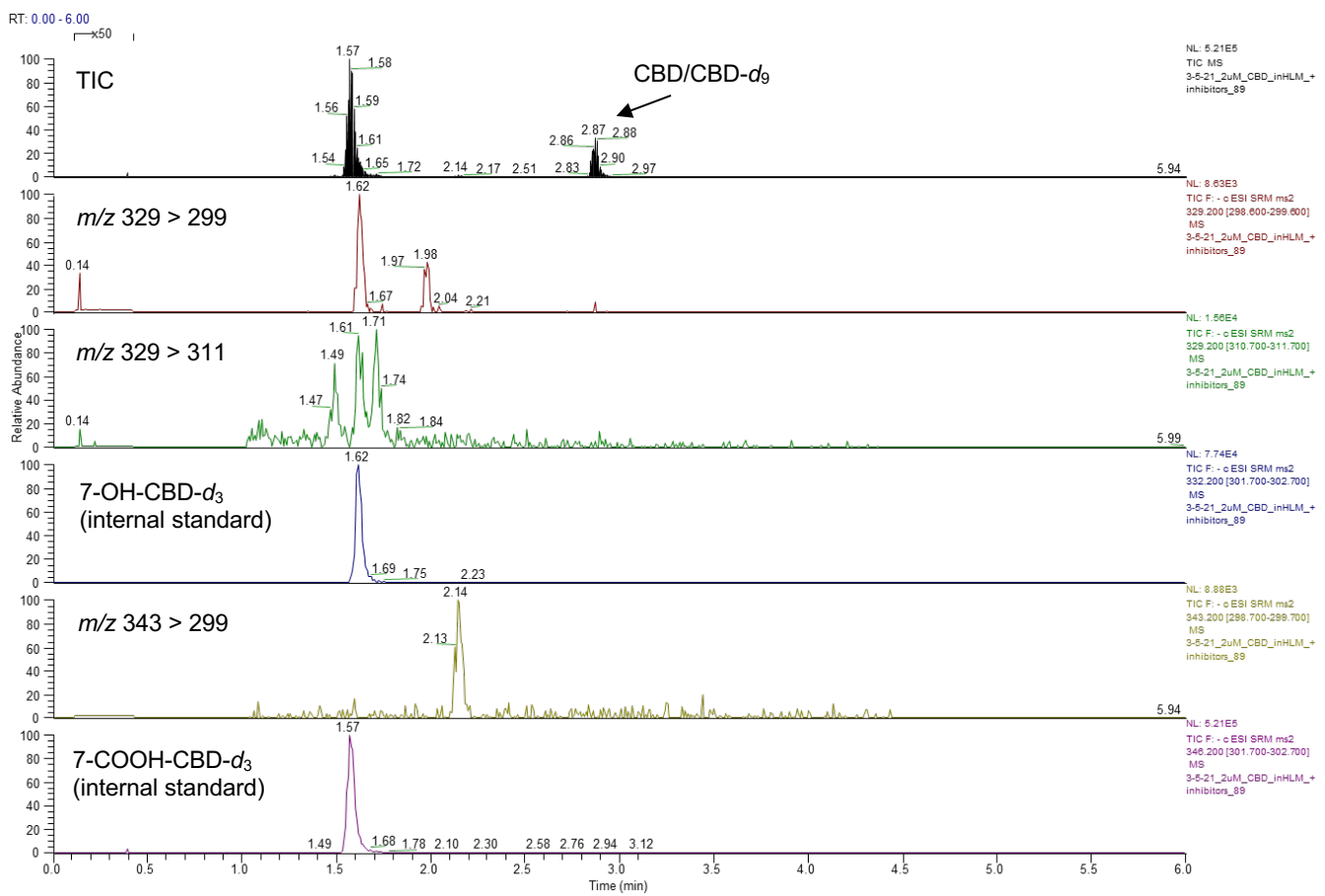
Supplemental Figure S3D. CBD (2 μ M) metabolism in HLM in the presence of furafylline. The total ion chromatogram (TIC) is shown (top) for all MRM transitions monitored. Mass transitions are as follows: 7-OH-CBD (1.61 min, m/z 329 > 299 and 329 > 311), M2 (1.95 min, m/z 329 > 299), 6 α -OH-CBD (1.48 min, m/z 329 > 311), M1 (1.7 min, m/z 329 > 311), 7-OH-CBD- d_3 (1.61 min, m/z 332 > 302), M3 (2.14 min, m/z 343 > 299), and 7-COOH-CBD- d_3 (1.57 min, m/z 346 > 302).



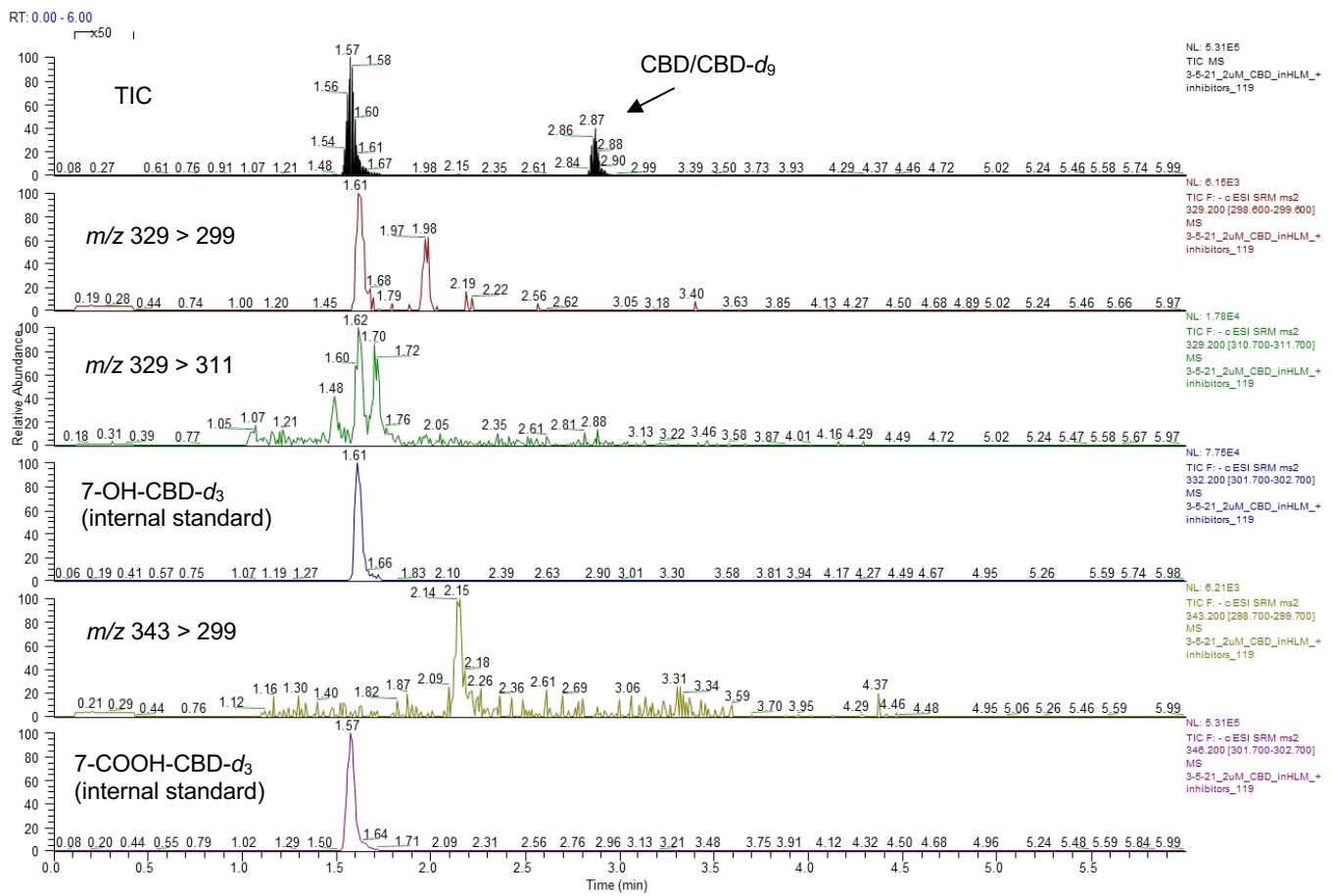
Supplemental Figure S3E. CBD (2 μ M) metabolism in HLM in the presence of PPP. The total ion chromatogram (TIC) is shown (top) for all MRM transitions monitored. Mass transitions are as follows: 7-OH-CBD (1.6 min, m/z 329 > 299 and 329 > 311), M2 (1.96 min, m/z 329 > 299), 6 α -OH-CBD (1.45 min, m/z 329 > 311), M1 (1.68 min, m/z 329 > 311), 7-OH-CBD- d_3 (1.58 min, m/z 332 > 302), M3 (2.13 min, m/z 343 > 299), and 7-COOH-CBD- d_3 (1.54 min, m/z 346 > 302).



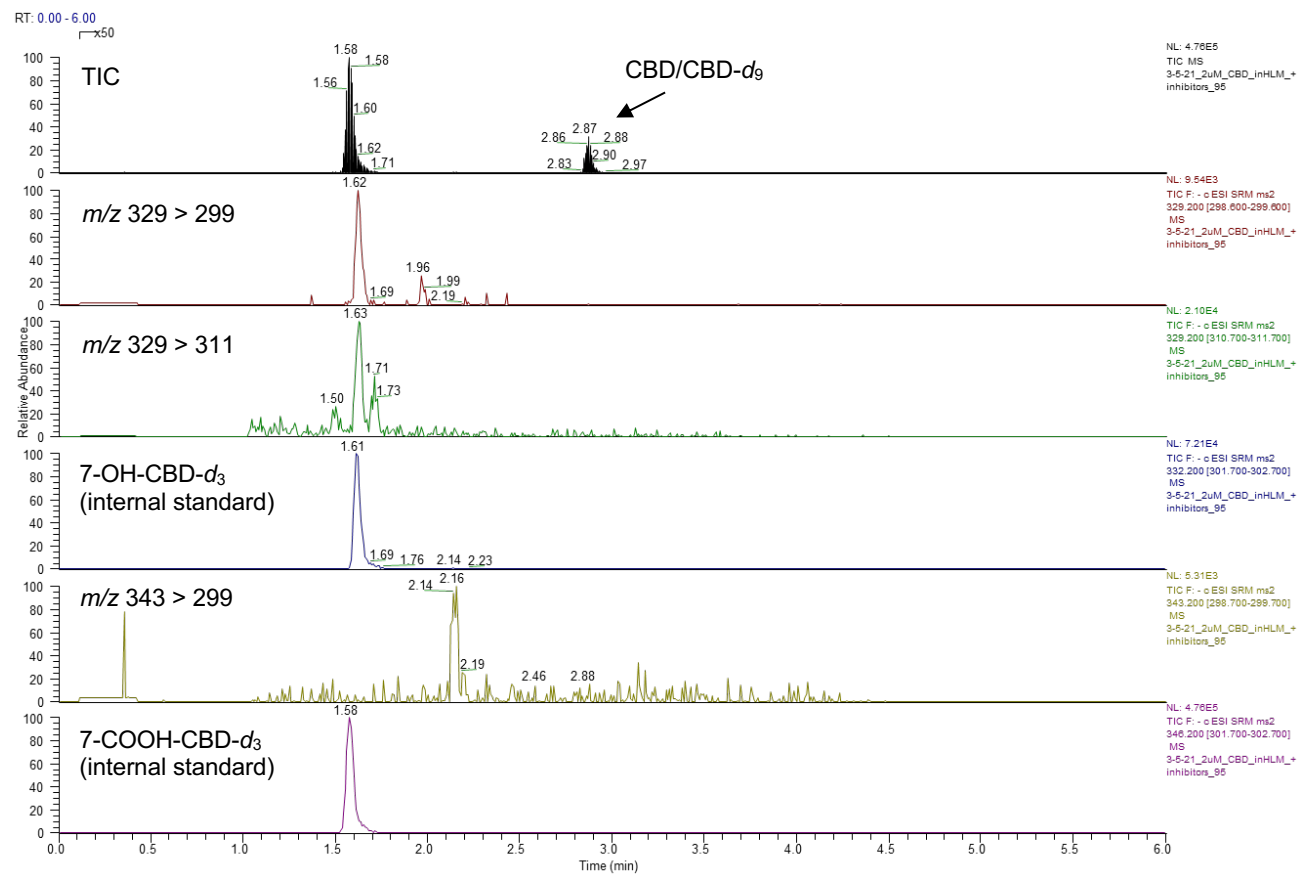
Supplemental Figure S3F. CBD (2 μM) metabolism in HLM in the presence of ticlopidine. The total ion chromatogram (TIC) is shown (top) for all MRM transitions monitored. Mass transitions are as follows: 7-OH-CBD (1.61 min, *m/z* 329 > 299 and 329 > 311), M2 (1.94 min, *m/z* 329 > 299), 6α-OH-CBD (1.48 min, *m/z* 329 > 311), M1 (1.69 min, *m/z* 329 > 311), 7-OH-CBD-*d*3 (1.60 min, *m/z* 332 > 302), M3 (2.13 min, *m/z* 343 > 299), and 7-COOH-CBD-*d*3 (1.56 min, *m/z* 346 > 302).



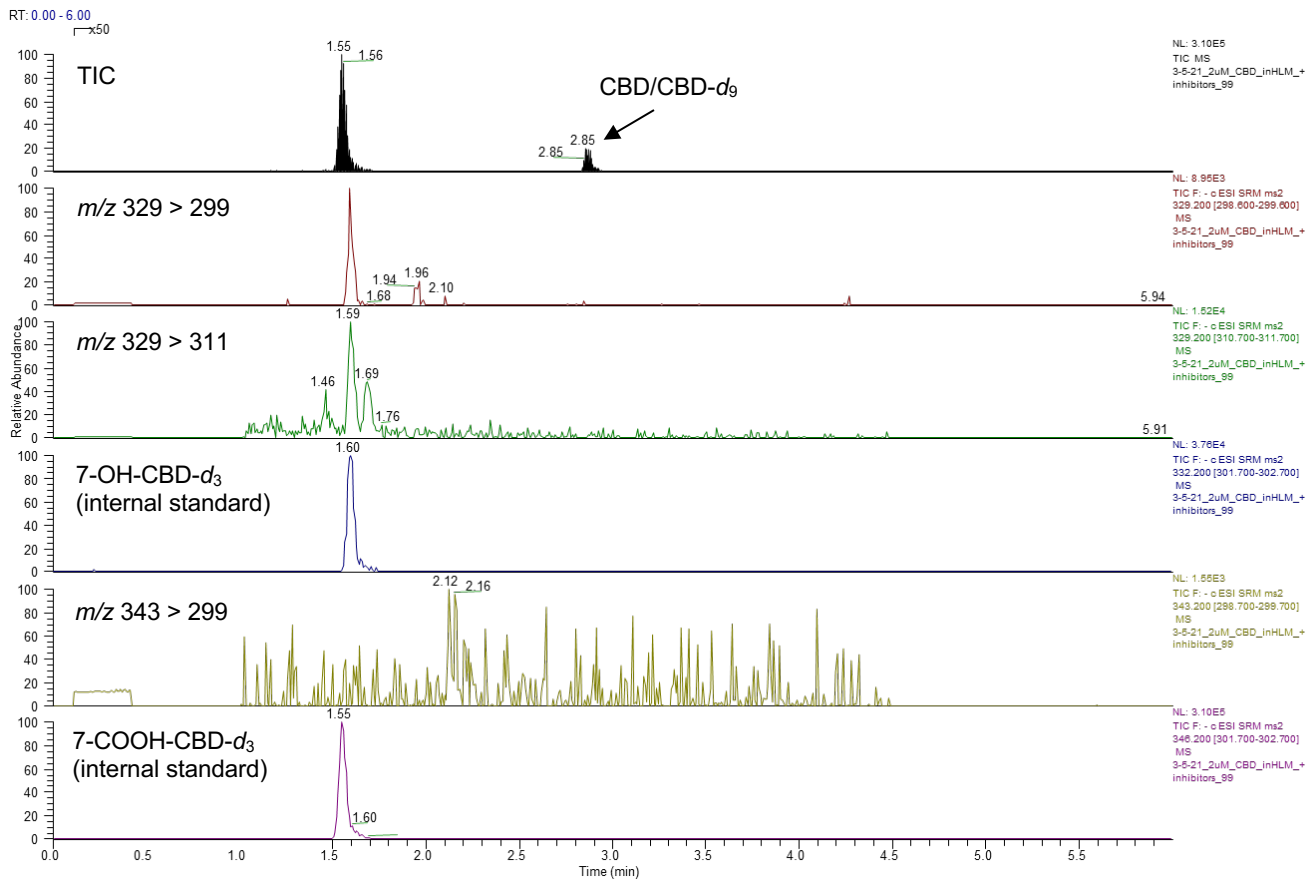
Supplemental Figure S3G. CBD (2 μ M) metabolism in HLM in the presence of sulfaphenazole. The total ion chromatogram (TIC) is shown (top) for all MRM transitions monitored. Mass transitions are as follows: 7-OH-CBD (1.62 min, m/z 329 > 299 and 329 > 311), M2 (1.98 min, m/z 329 > 299), 6 α -OH-CBD (1.49 min, m/z 329 > 311), M1 (1.71 min, m/z 329 > 311), 7-OH-CBD- d_3 (1.62 min, m/z 332 > 302), M3 (2.14 min, m/z 343 > 299), and 7-COOH-CBD- d_3 (1.57 min, m/z 346 > 302).



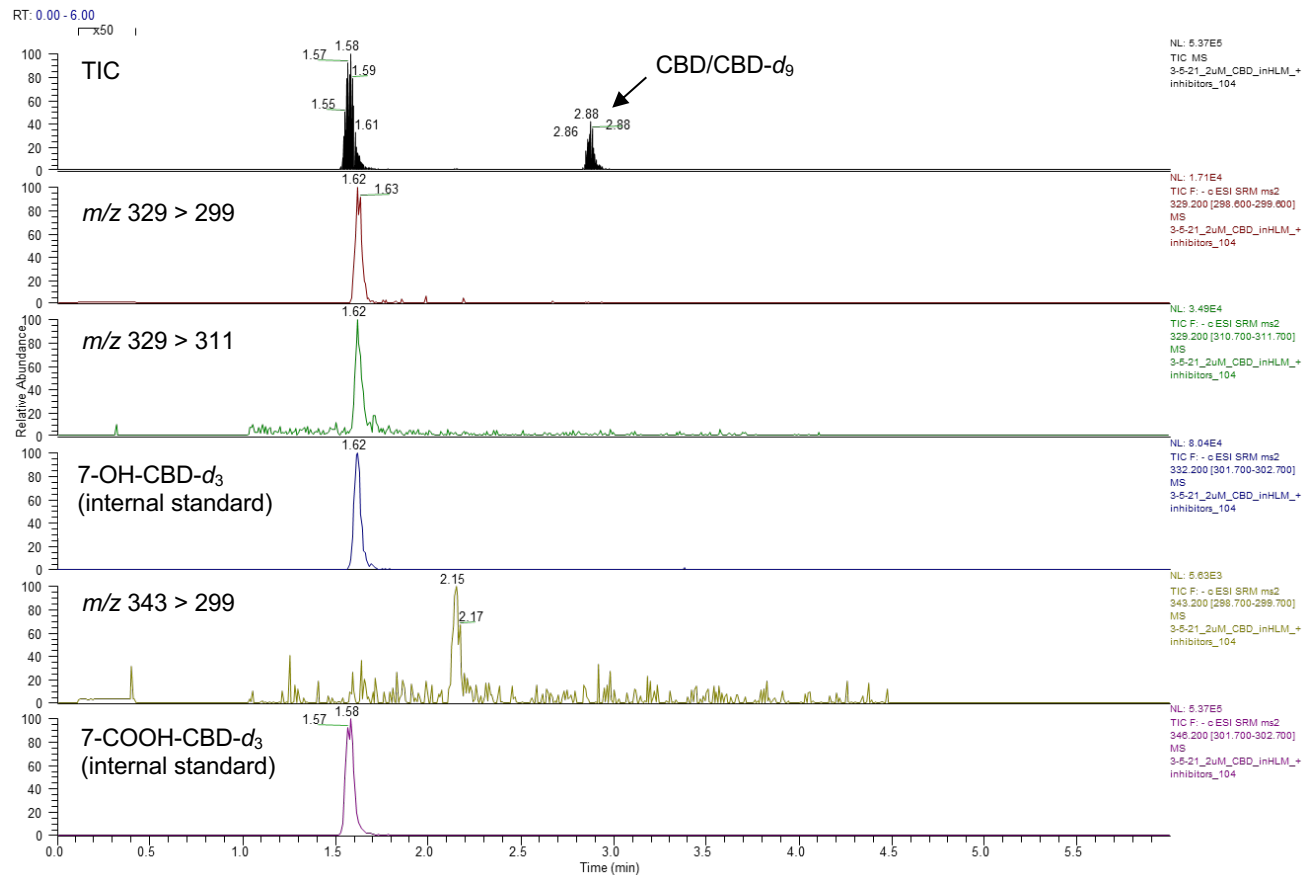
Supplemental Figure S3H. CBD (2 μ M) metabolism in HLM in the presence of benzylnirvanol. Mass transitions are as follows: 7-OH-CBD (1.61 min, m/z 329 > 299 and 329 > 311), M2 (1.98 min, m/z 329 > 299), 6 α -OH-CBD (1.48 min, m/z 329 > 311), M1 (1.70 min, m/z 329 > 311), 7-OH-CBD-d₃ (1.61 min, m/z 332 > 302), M3 (2.15 min, m/z 343 > 299), and 7-COOH-CBD-d₃ (1.57 min, m/z 346 > 302).



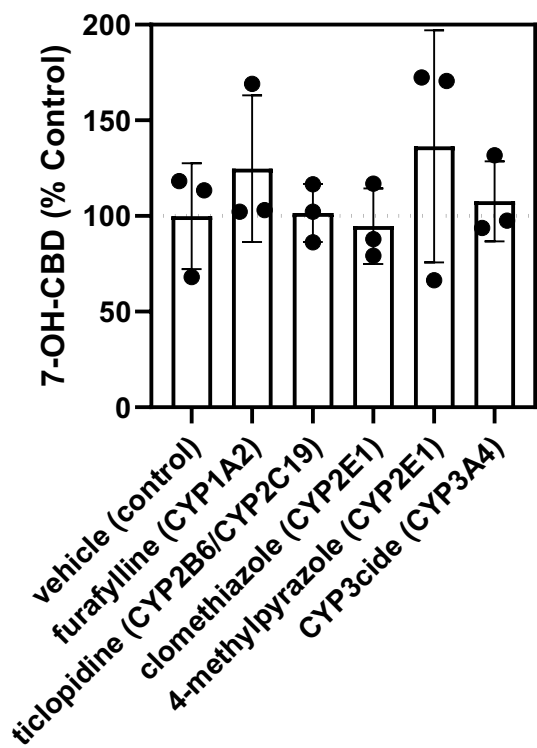
Supplemental Figure S3I. CBD (2 μ M) metabolism in HLM in the presence of quinidine. Mass transitions are as follows: 7-OH-CBD (1.62 min, m/z 329 > 299 and 329 > 311), M2 (1.96 min, m/z 329 > 299), 6 α -OH-CBD (1.50 min, m/z 329 > 311), M1 (1.71 min, m/z 329 > 311), 7-OH-CBD-d₃ (1.61 min, m/z 332 > 302), M3 (2.16 min, m/z 343 > 299), and 7-COOH-CBD-d₃ (1.58 min, m/z 346 > 302).



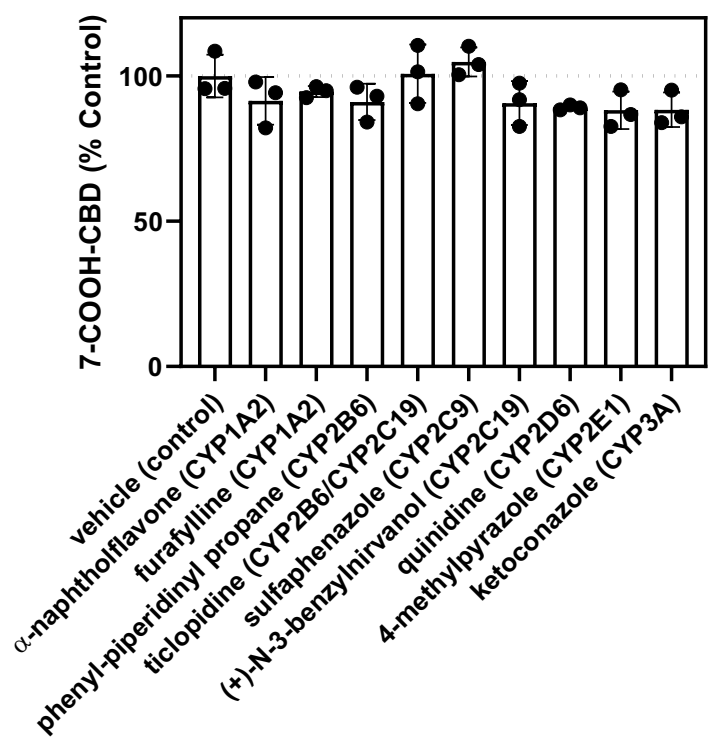
Supplemental Figure S3J. CBD (2 μ M) metabolism in HLM in the presence of 4-methylpyrazole. Mass transitions are as follows: 7-OH-CBD (1.59 min, m/z 329 > 299 and 329 > 311), M2 (1.96 min, m/z 329 > 299), 6 α -OH-CBD (1.46 min, m/z 329 > 311), M1 (1.69 min, m/z 329 > 311), 7-OH-CBD-d₃ (1.6 min, m/z 332 > 302), and 7-COOH-CBD-d₃ (1.55 min, m/z 346 > 302).



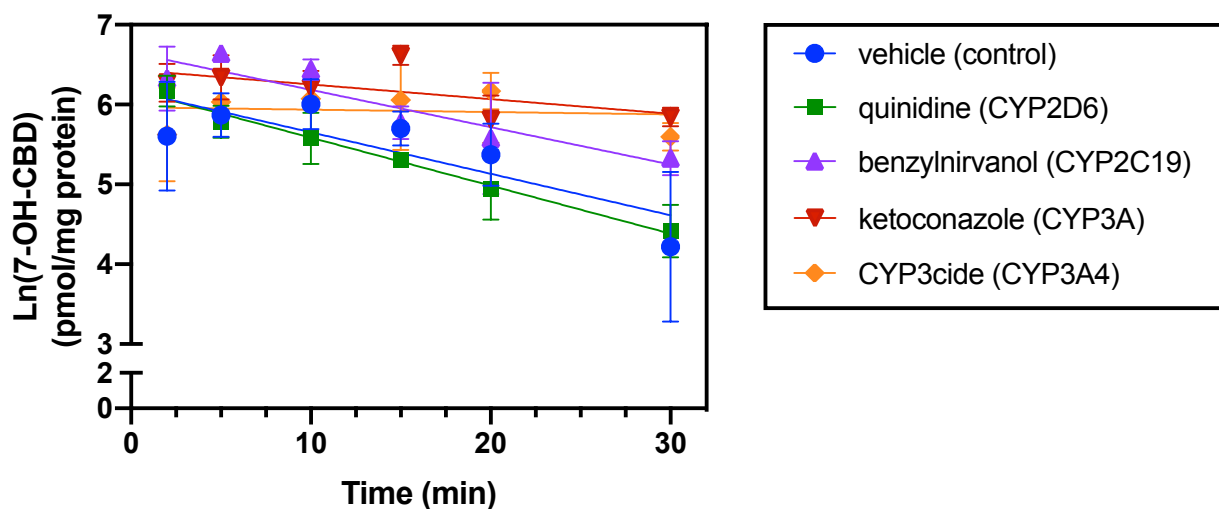
Supplemental Figure S3K. CBD (2 μ M) metabolism in HLM in the presence of ketoconazole. Mass transitions are as follows: 7-OH-CBD (1.62 min, m/z 329 > 299 and 329 > 311), 7-OH-CBD-d₃ (1.62 min, m/z 332 > 302), M3 (2.15 min, m/z 343 > 299), and 7-COOH-CBD-d₃ (1.57 min, m/z 346 > 302).



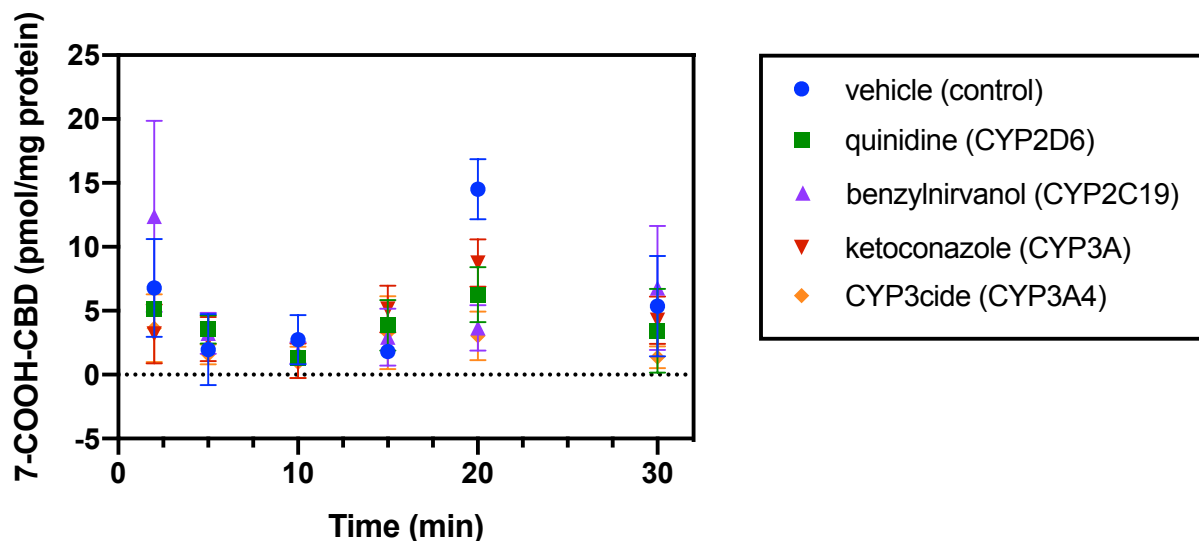
Supplemental Figure S4. 7-OH-CBD formation in the presence of time-dependent CYP-selective inhibitors. CBD (1 μ M) was incubated in 150-donor pooled HLM (0.2 mg/mL protein) in the presence of the following time-dependent inhibitors: CYP3cide (0.5 μ M), furafylline (25 μ M), clomethiazole (30 μ M), ticlopidine (5 μ M), 4-methylpyrazole (100 μ M) or vehicle. Metabolite formation was determined by LC-MS/MS analysis and is expressed as a percentage relative to incubations containing vehicle control. Points represent the mean \pm SD of a single experiment performed in triplicate.



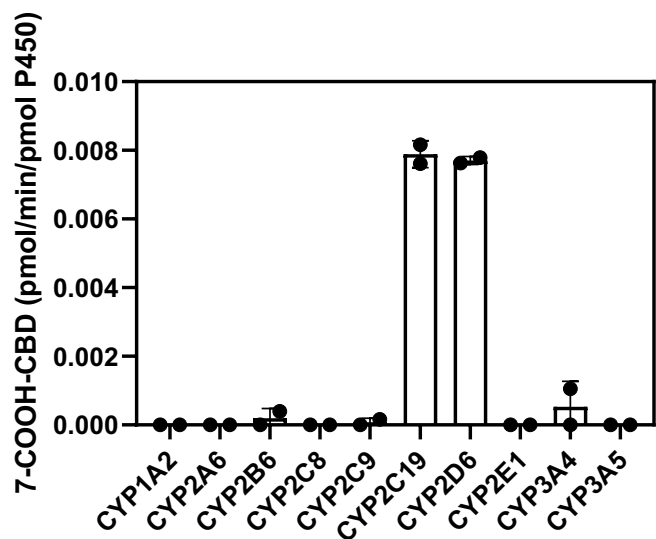
Supplemental Figure S5. Effect of CYP-selective chemical inhibitors on 7-OH-CBD metabolism. 7-OH-CBD (2 μ M) was incubated with pooled HLM (0.2 mg/mL protein) for 10 min. Formation of 7-COOH-CBD was measured in the presence of CYP-selective inhibitors and compared to vehicle control incubations. Rates of metabolite formation were calculated using a standard curve in the range of 5-500 ng/mL (limit of quantitation = 10 ng/mL for 7-COOH-CBD). The rate of 7-COOH-CBD formation with vehicle control was below the limit of quantitation for this experiment; results were therefore interpreted by comparing peak area ratios with respect to internal standard (7-COOH-CBD-d₃). The affected enzyme(s) for each inhibitor are listed in parentheses. Bars represent the mean \pm SD of a single experiment performed in triplicate.



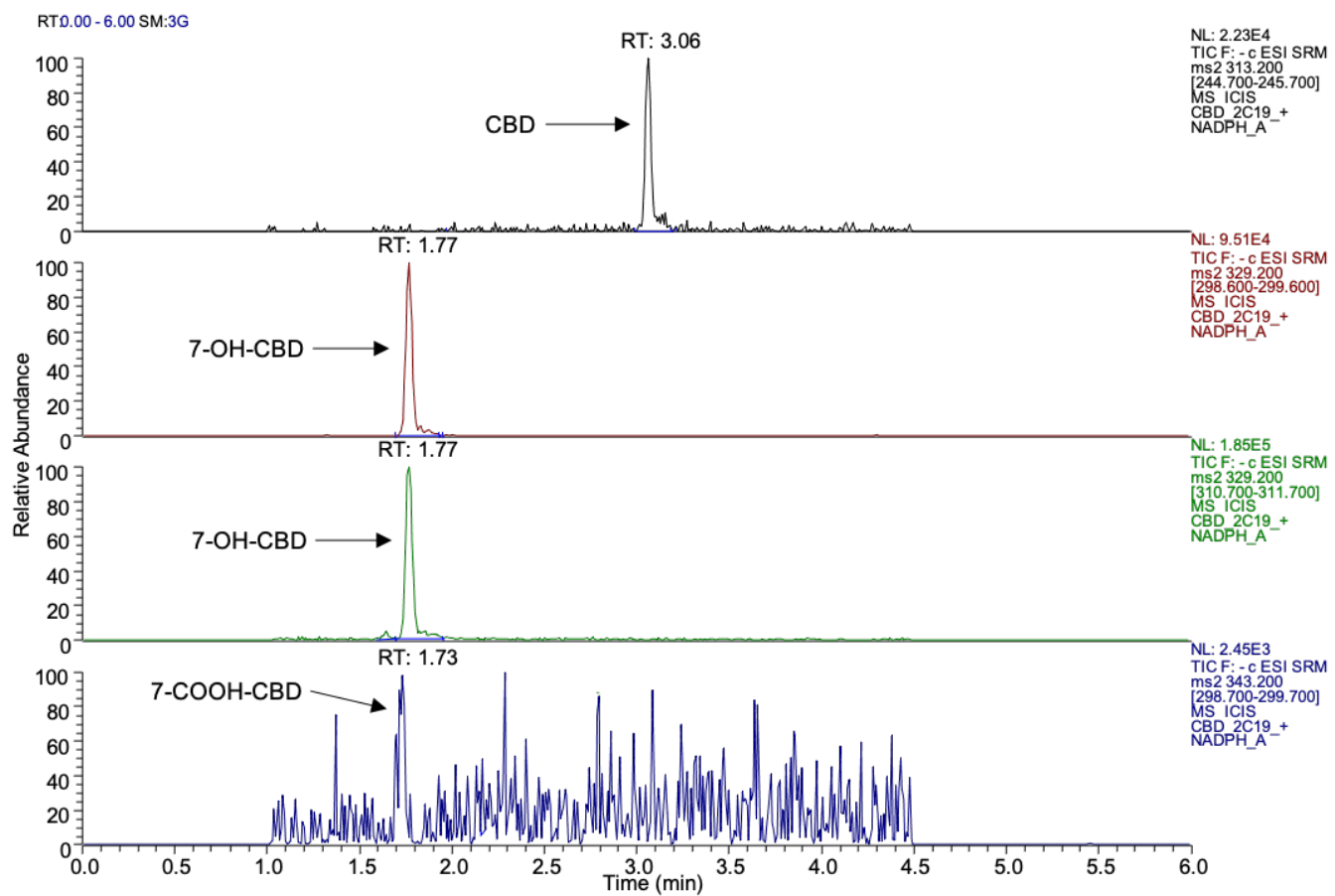
Supplemental Figure S6A. Effect of CYP2C19, CYP2D6, and CYP3A inhibition on 7-OH-CBD depletion. 7-OH-CBD (1 μ M) was incubated with 150-donor pooled HLM (0.2 mg/mL protein) in the presence of vehicle control, quinidine (2 μ M), (+)-N-benzylnirvanol (5 μ M), ketoconazole (1 μ M), and CYP3cide (0.5 μ M) for 2, 5, 10, 15, 20, and 30 min. For reactions containing the time-dependent inhibitor CYP3cide, a 10-minute preincubation with CYP3cide and HLM was performed prior to addition of 7-OH-CBD. The rate of 7-OH-CBD depletion was calculated using log-transformed values over 30 min. Analyte quantitation was performed using a standard curve ranging from 1-500 ng/mL (limit of quantitation = 1 ng/mL). Points represent the mean \pm SD of a single experiment performed in triplicate.



Supplemental Figure S6B. Effect of CYP2C19, CYP2D6, and CYP3A inhibition on 7-COOH-CBD formation. 7-OH-CBD (1 μ M) was incubated with 150-donor pooled HLM (0.2 mg/mL protein) in the presence of vehicle control, quinidine (2 μ M), (+)-*N*-benzylnirvanol (5 μ M), ketoconazole (1 μ M), and CYP3cide (0.5 μ M) for 2, 5, 10, 15, 20, and 30 min. For reactions containing the time-dependent inhibitor CYP3cide, a 10-minute preincubation with CYP3cide and HLM was performed prior to addition of 7-OH-CBD. Formation of 7-COOH-CBD was measured by LC-MS/MS using an authentic standard. Points represent the mean \pm SD of a single experiment conducted in triplicate.

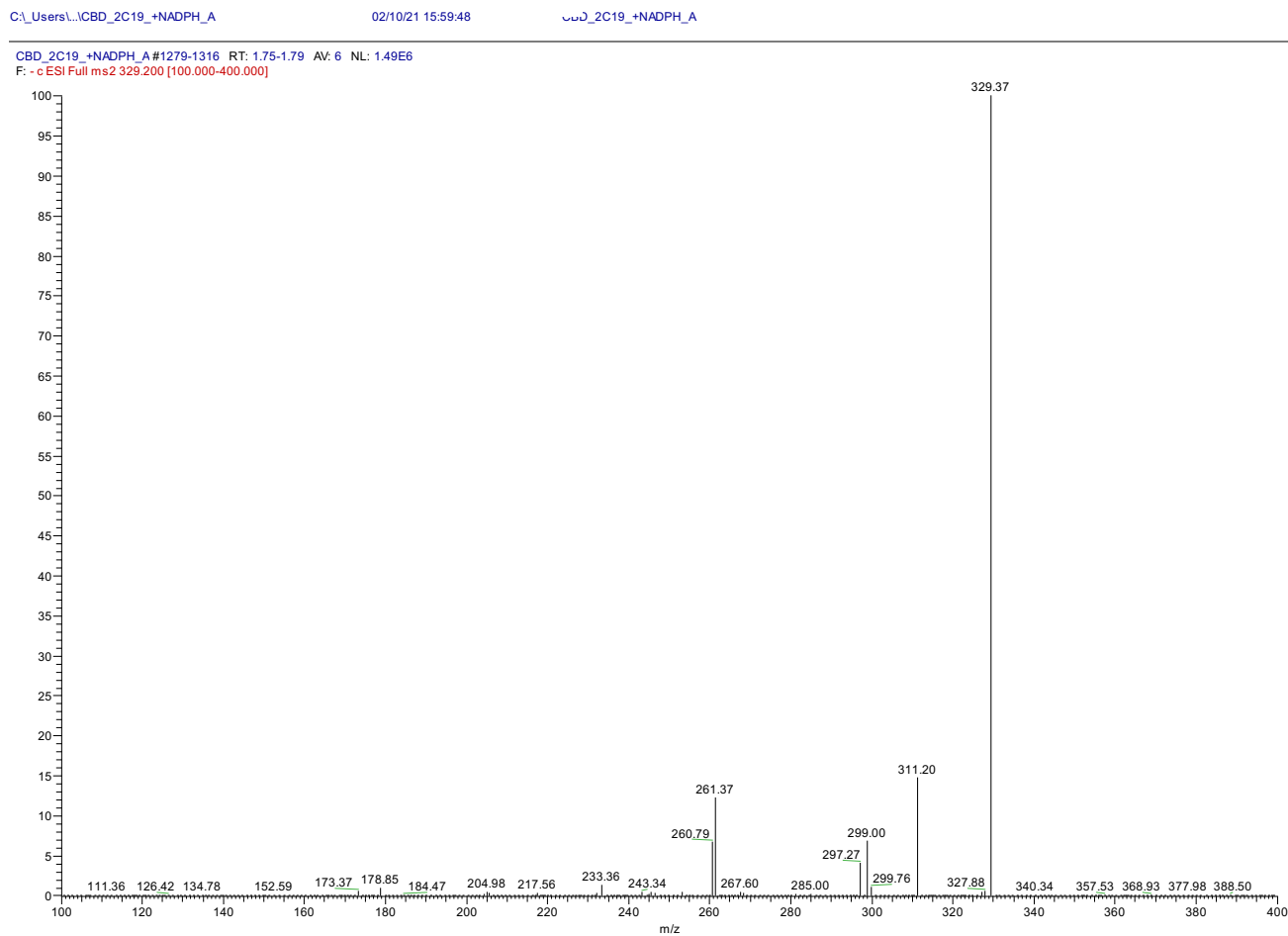


Supplemental Figure S7. Metabolism of 7-OH-CBD by recombinant CYP enzymes. 7-OH-CBD (2 μ M) was incubated with CYP SupersomesTM (20 pmol/mL) for 10 min. Formation of 7-COOH-CBD was measured by LC-MS/MS analysis and extrapolated from a 7-COOH-CBD standard curve in the range of 1-500 ng/mL (limit of quantitation = 5 ng/mL). Bars represent the mean \pm SD of two experiments performed in triplicate.

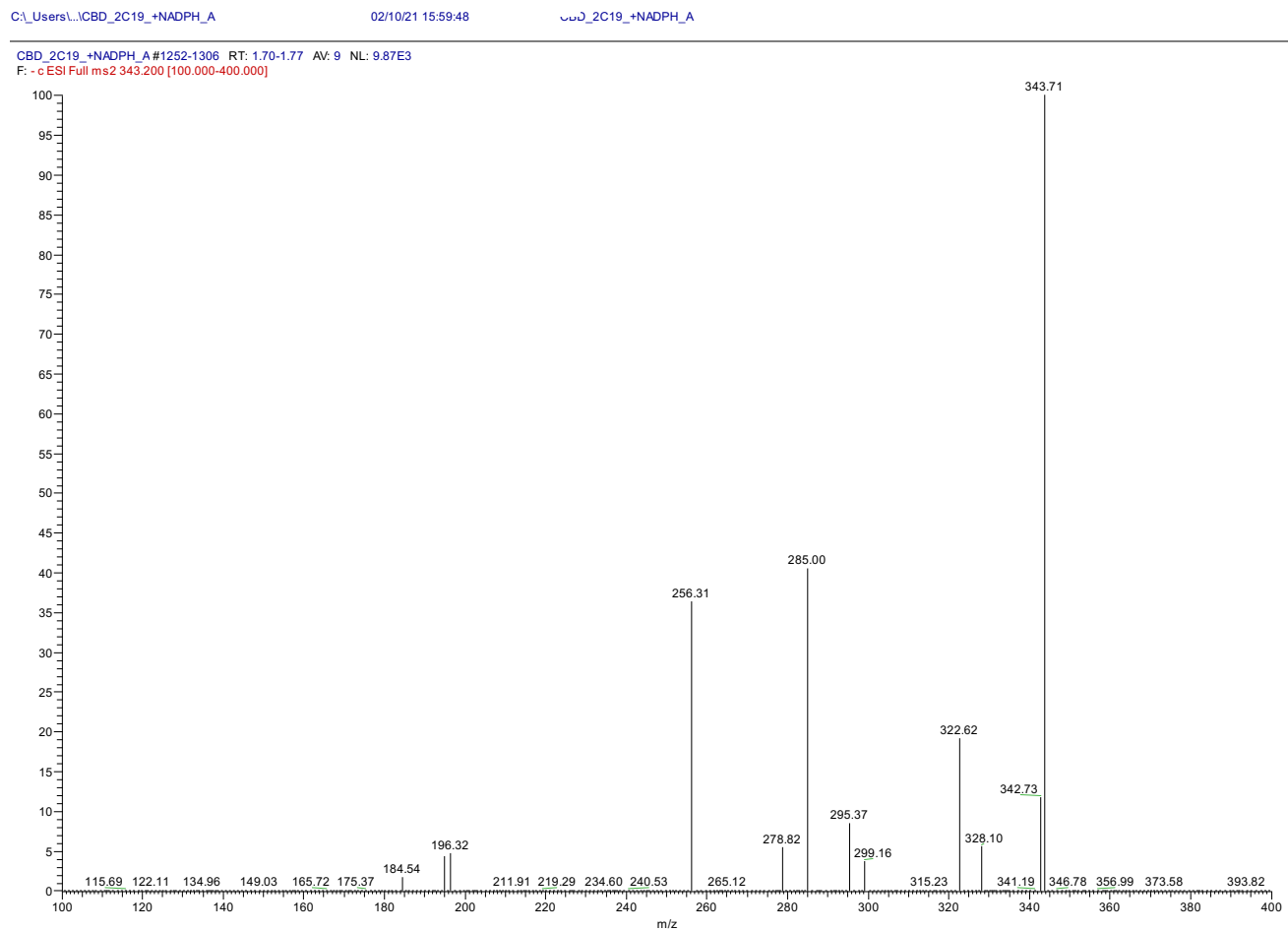


Supplemental Figure S8A. Representative LC-MS/MS chromatogram of CBD metabolites

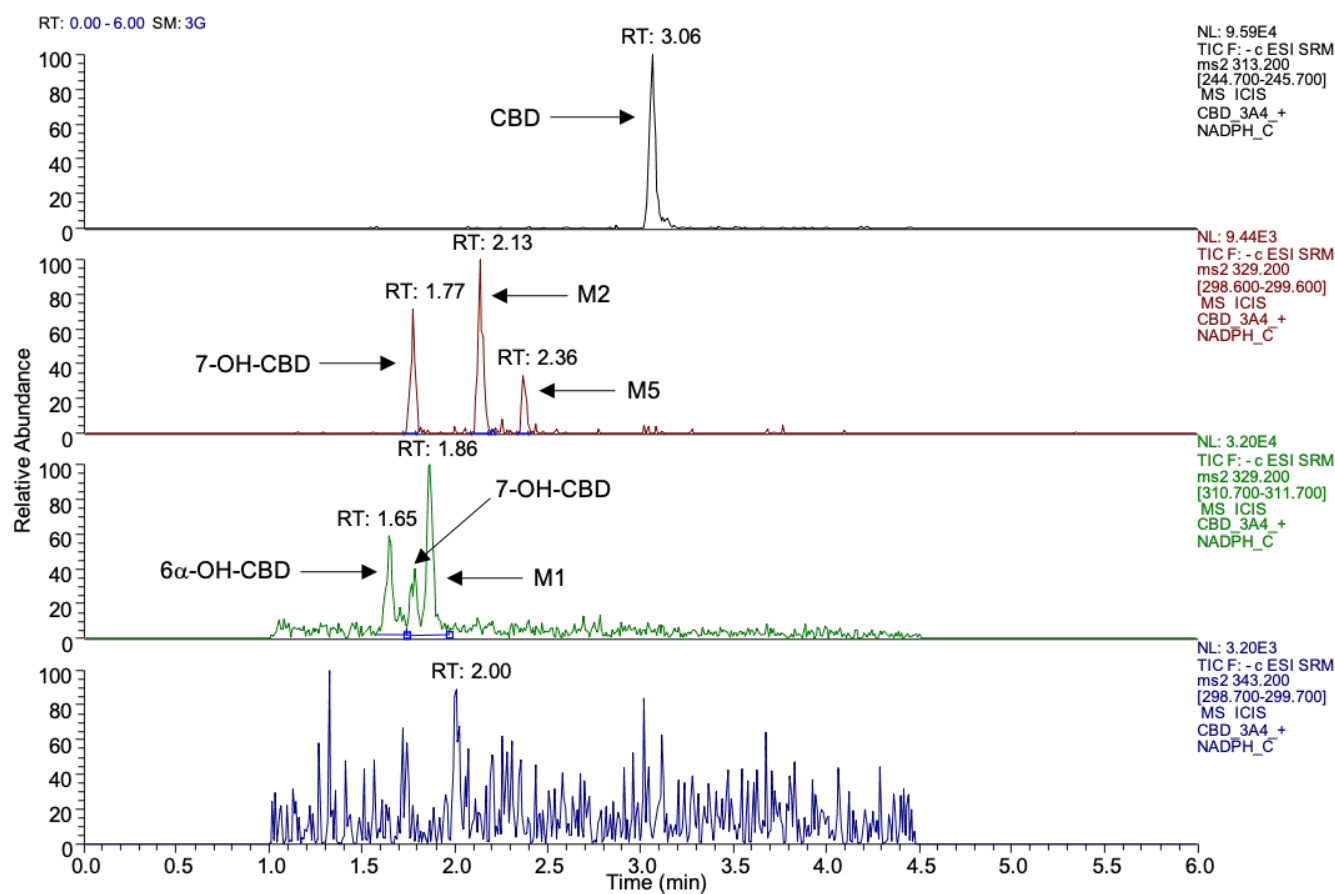
formed by recombinant CYP2C19. CBD (10 μ M) was incubated with recombinant CYP2C19 (20 pmol/mL) for 10 min in the presence of NADPH. CBD metabolites were measured by LC-MS/MS analysis using multiple reaction monitoring (MRM). The following precursor-to-product ion transitions were used for detection in the negative ion mode: CBD (m/z 313 > 245), 7-OH-CBD (retention time 1.77 min, m/z 329 > 299 and m/z 329 > 311), and 7-COOH-CBD (retention time 1.73 min, m/z 343 > 299).



Supplemental Figure S8B. Product ion spectrum of 7-OH-CBD formed in rCYP2C19 (m/z 329).



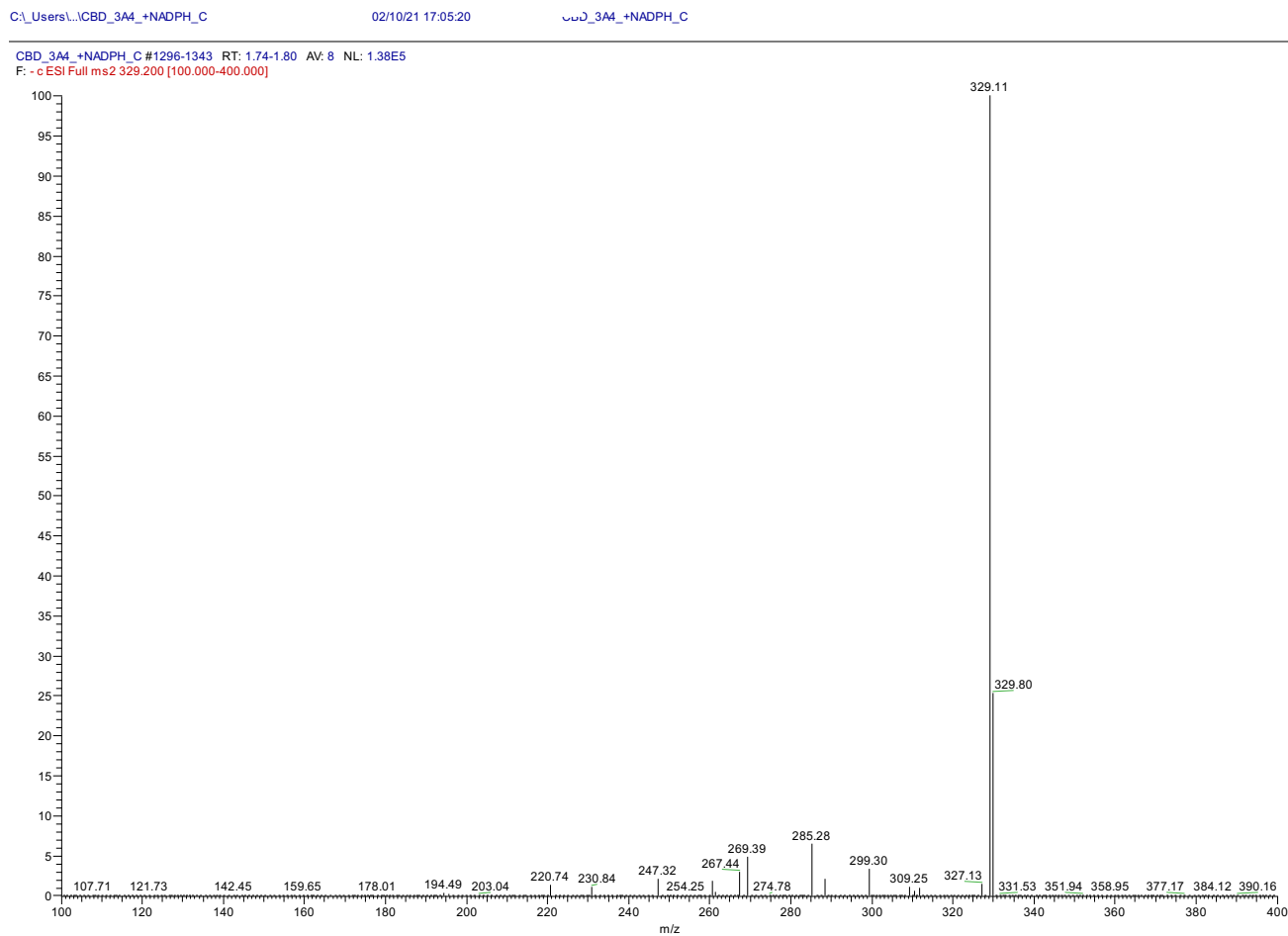
Supplemental Figure S8C. Product ion spectrum of 7-COOH-CBD formed in rCYP2C19 (m/z 343).



Supplemental Figure S9A. Representative LC-MS/MS chromatogram of CBD metabolites

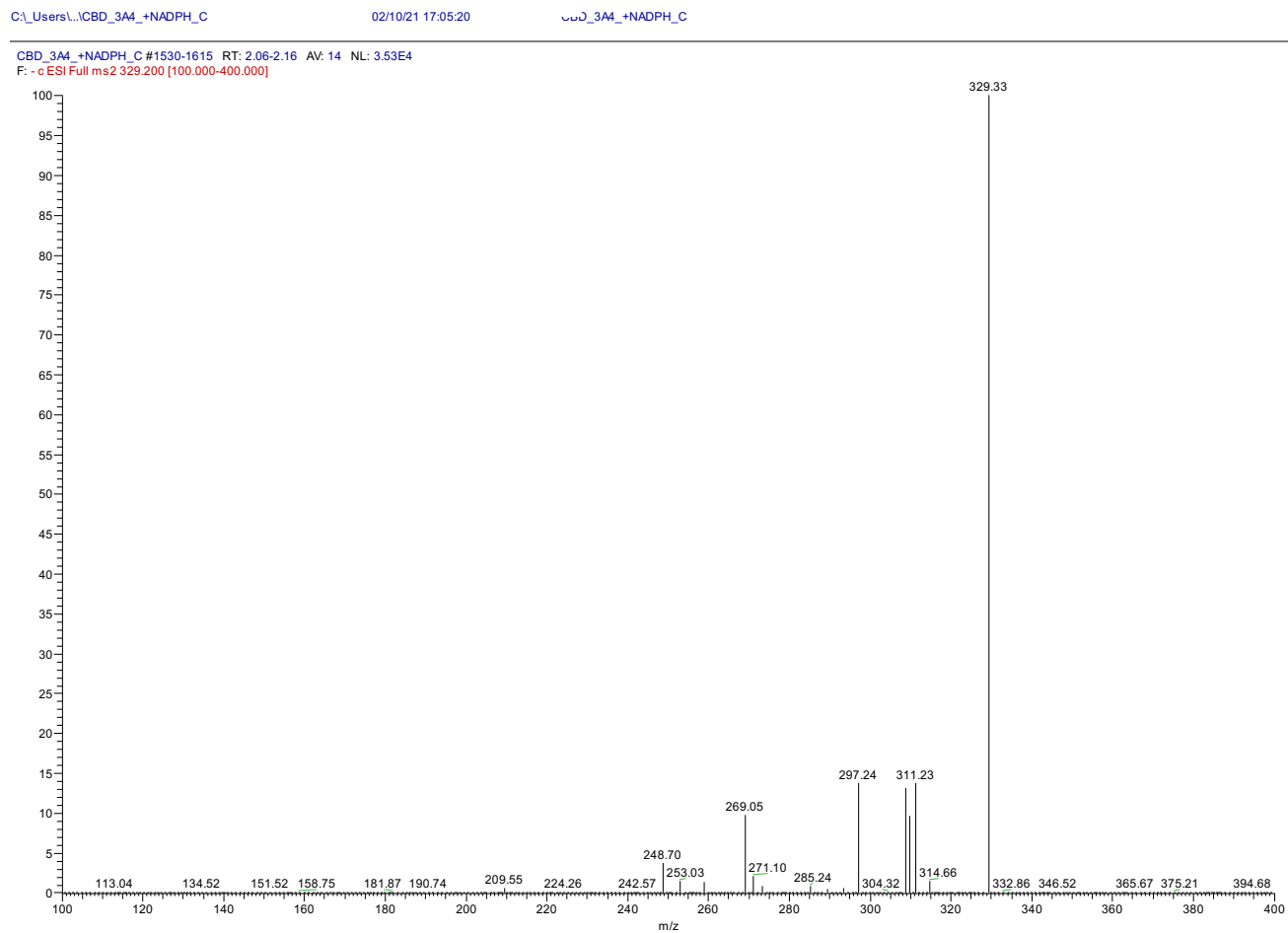
formed by recombinant CYP3A4. CBD (10 μ M) was incubated with recombinant CYP3A4 (20 pmol/mL) for 10 min in the presence of NADPH. CBD metabolites were measured by LC-MS/MS analysis using multiple reaction monitoring (MRM). The following precursor-to-product ion transitions were used for detection in the negative ion mode: CBD (m/z 313 $>$ 245), 7-OH-CBD (retention time 1.77 min, m/z 329 $>$ 299 and m/z 329 $>$ 311), and 7-COOH-CBD (retention time 1.73 min, m/z 343 $>$ 299), 6 α -OH-CBD (retention time 1.65 min, m/z 329 $>$ 311), and M1 (retention time 1.86 min, m/z 329 $>$ 311), M2 (retention time 2.13 min, m/z 329 $>$ 299), M4 (retention time 2.00 min, m/z 343 $>$ 299), and M5 (retention time 2.36 min, m/z 329 $>$ 299). Unknown

DMD-AR-2020-000350R2



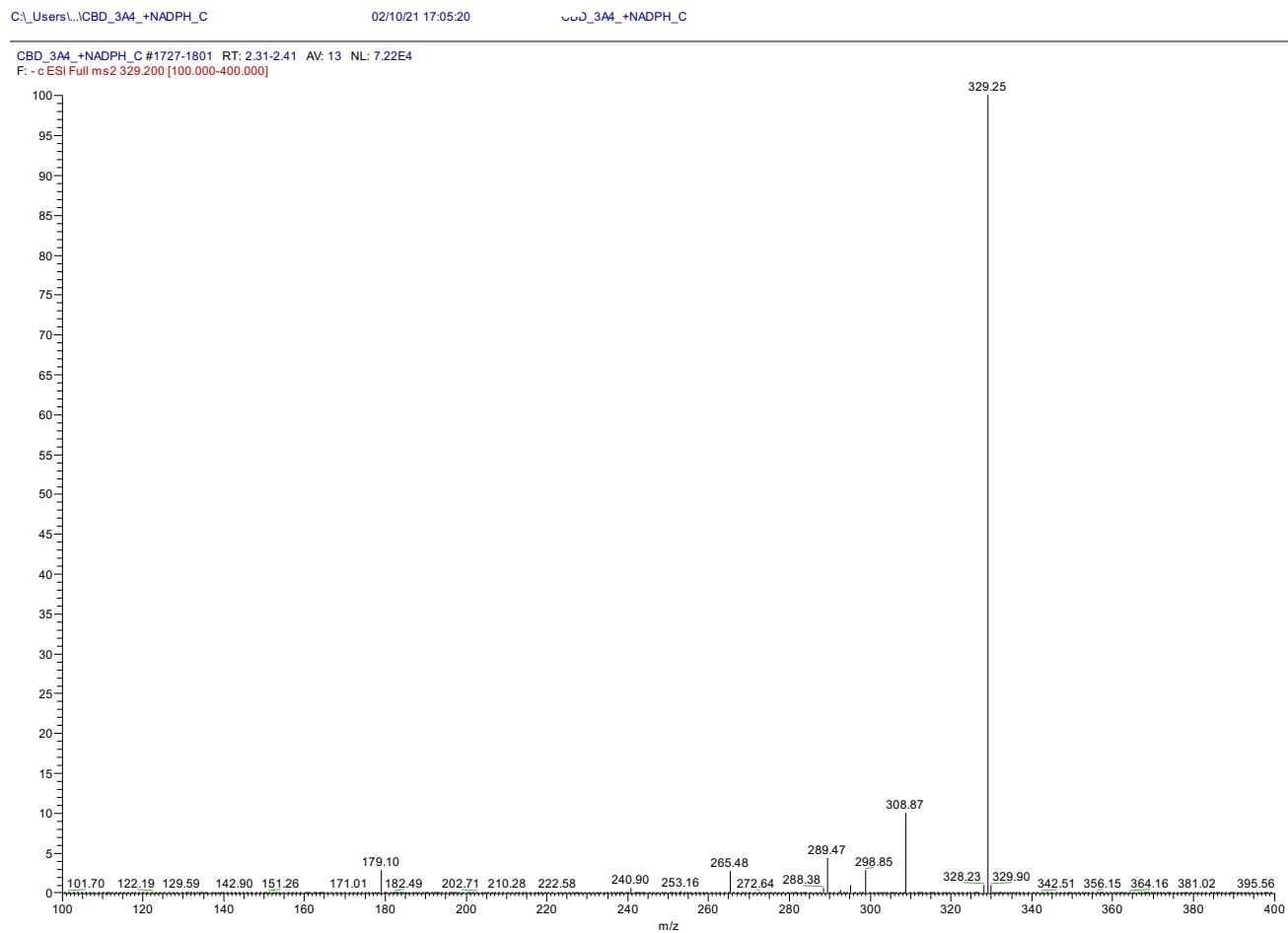
Supplemental Figure S9B. Product ion spectrum of 7-OH-CBD formed in rCYP3A4 (m/z 329).

DMD-AR-2020-000350R2

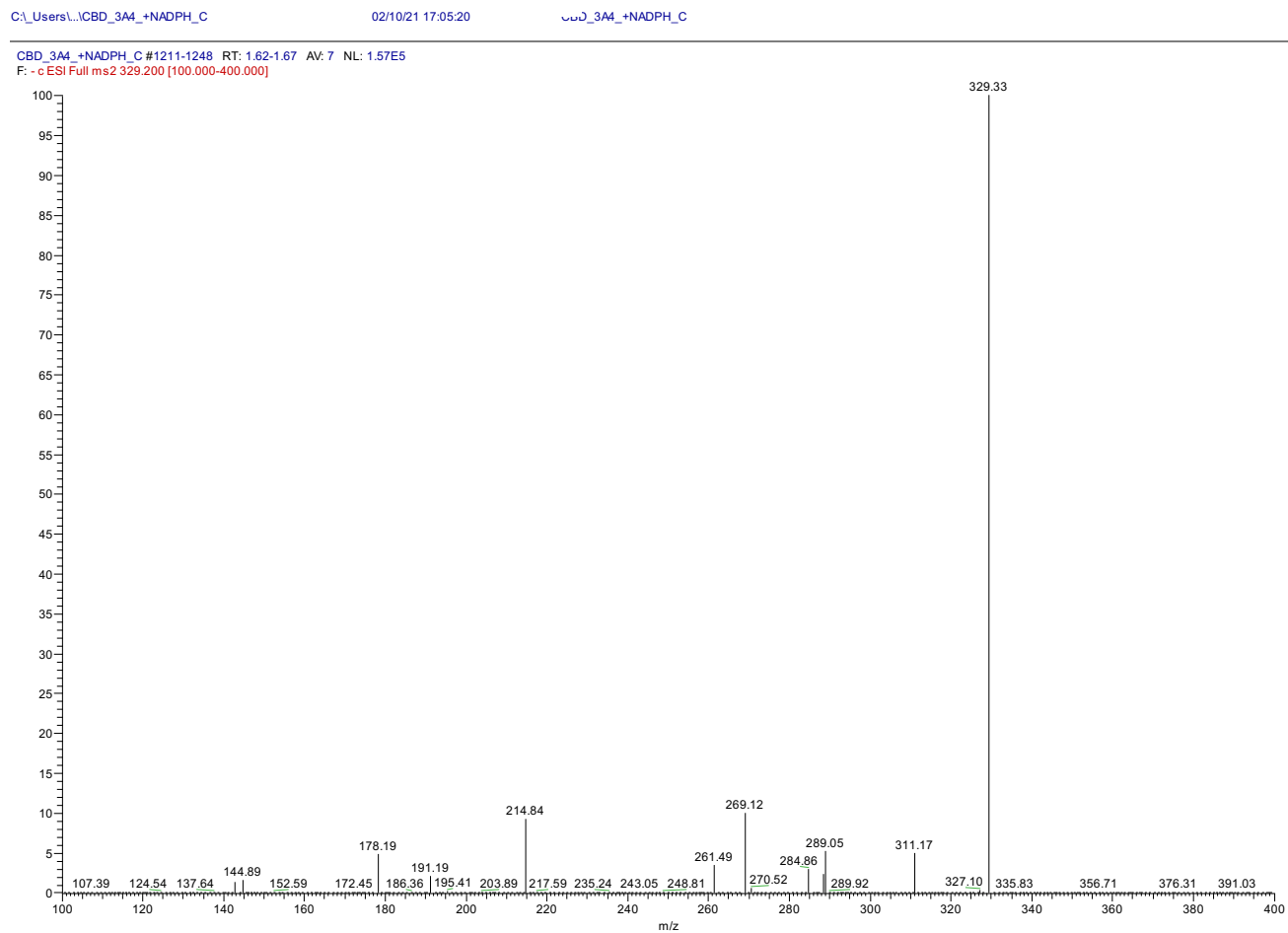


Supplemental Figure S9C. Product ion spectrum of M2 formed in rCYP3A4 (m/z 329).

DMD-AR-2020-000350R2

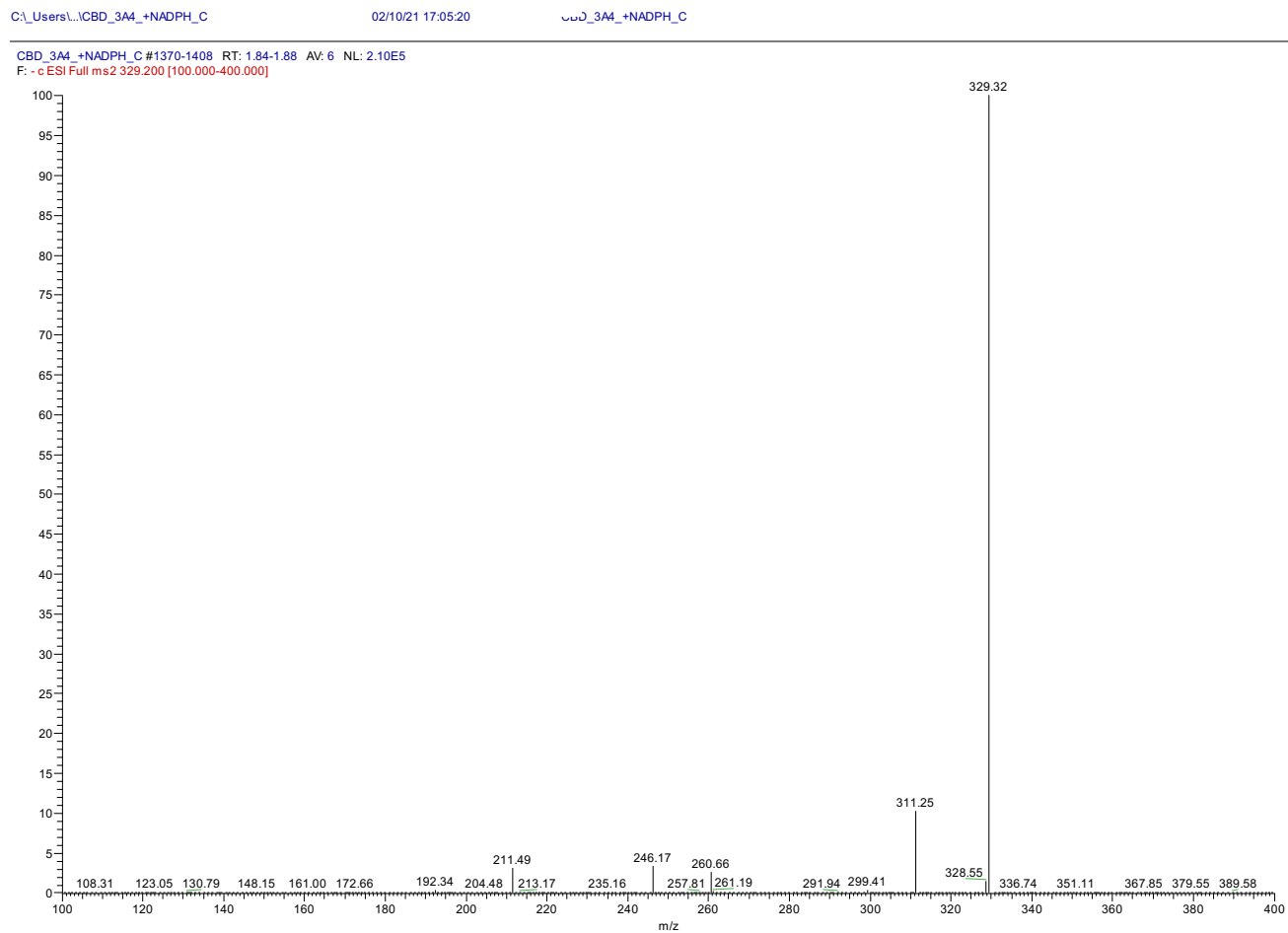


Supplemental Figure S9D. Product ion spectrum of M5 formed in rCYP3A4 (m/z 329).



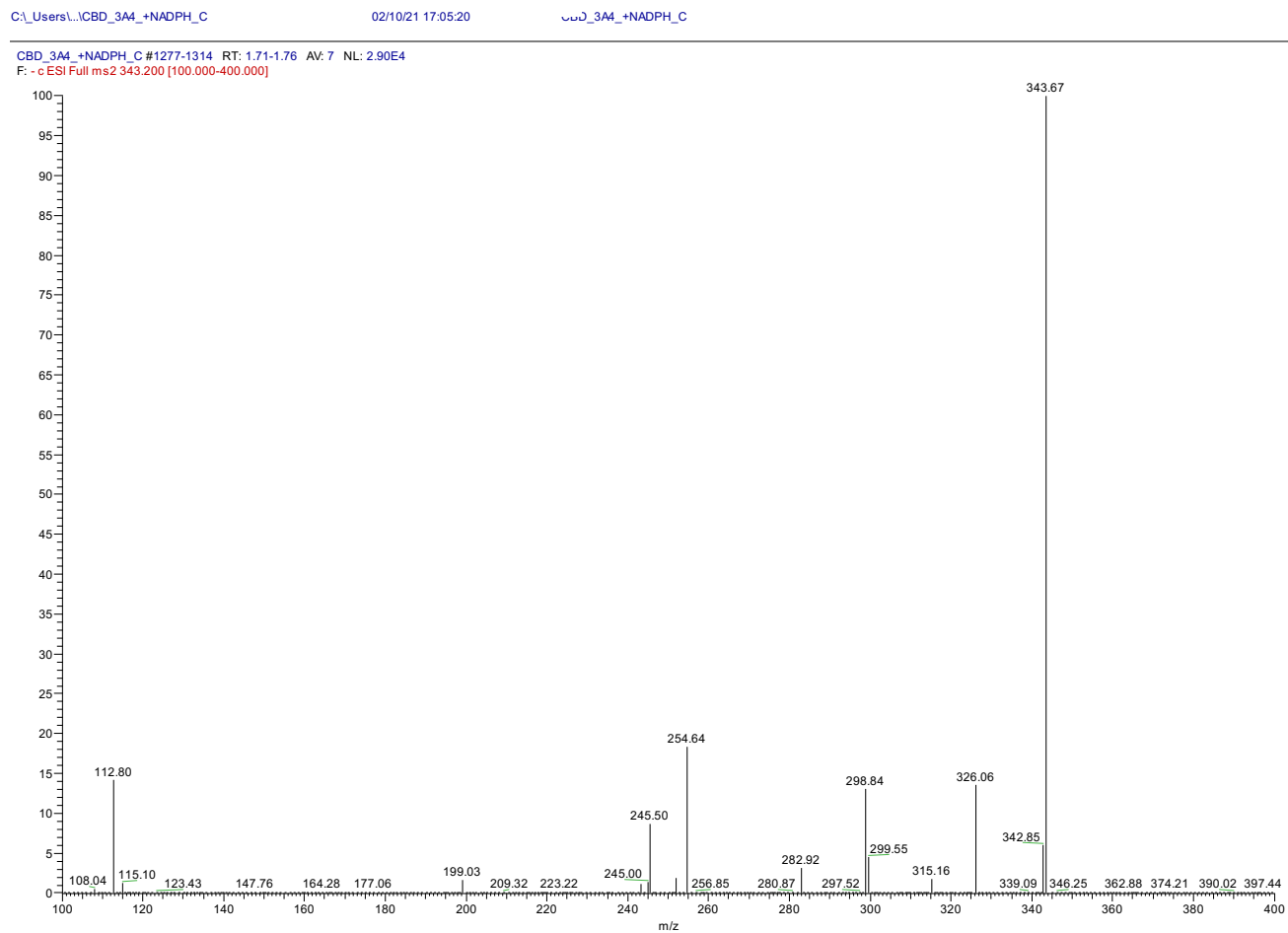
Supplemental Figure S9E. Product ion spectrum of 6 α -OH-CBD formed in rCYP3A4 (m/z 329).

DMD-AR-2020-000350R2



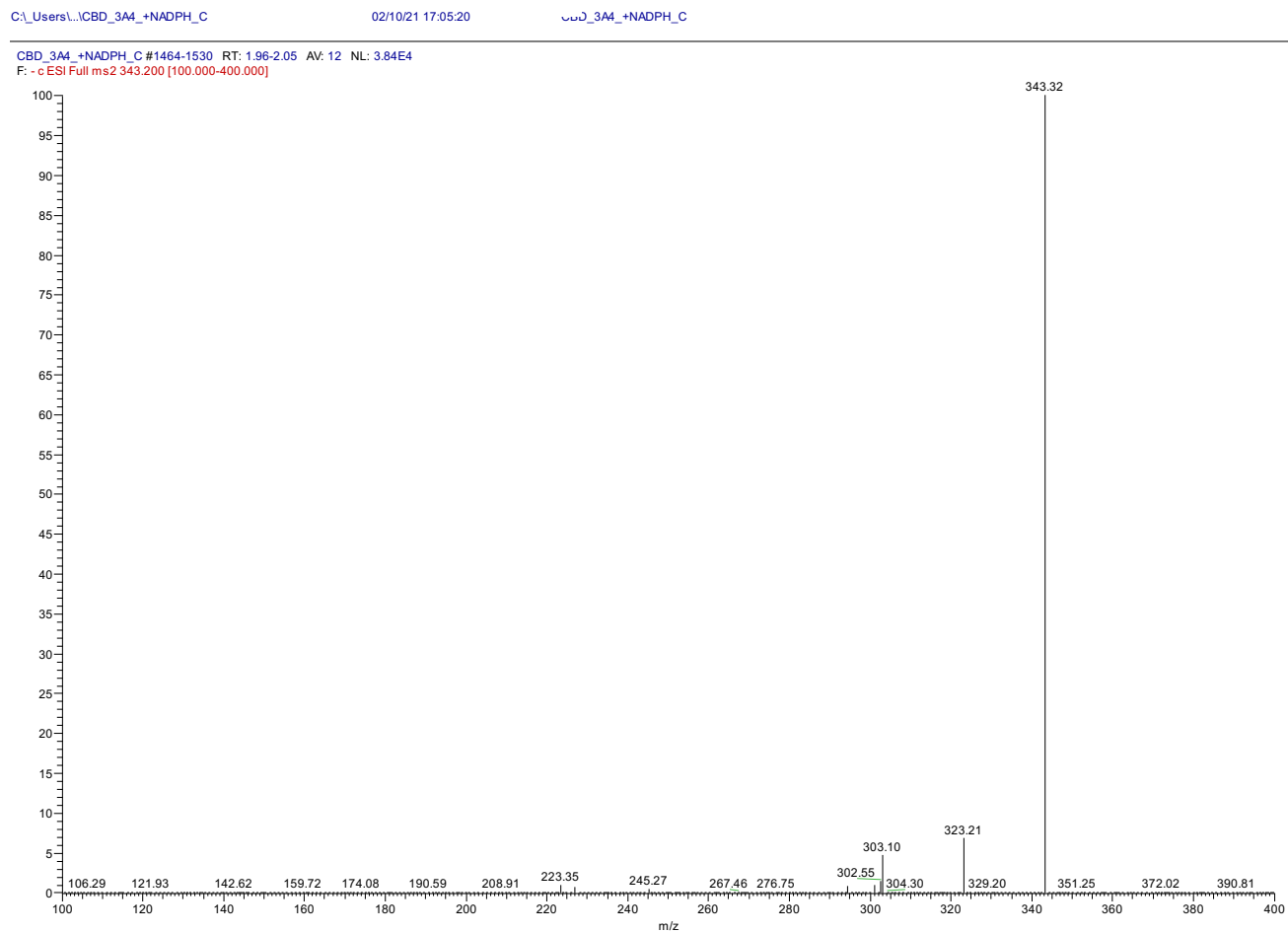
Supplemental Figure S9F. Product ion spectrum of M1 formed in rCYP3A4 (m/z 329).

DMD-AR-2020-000350R2

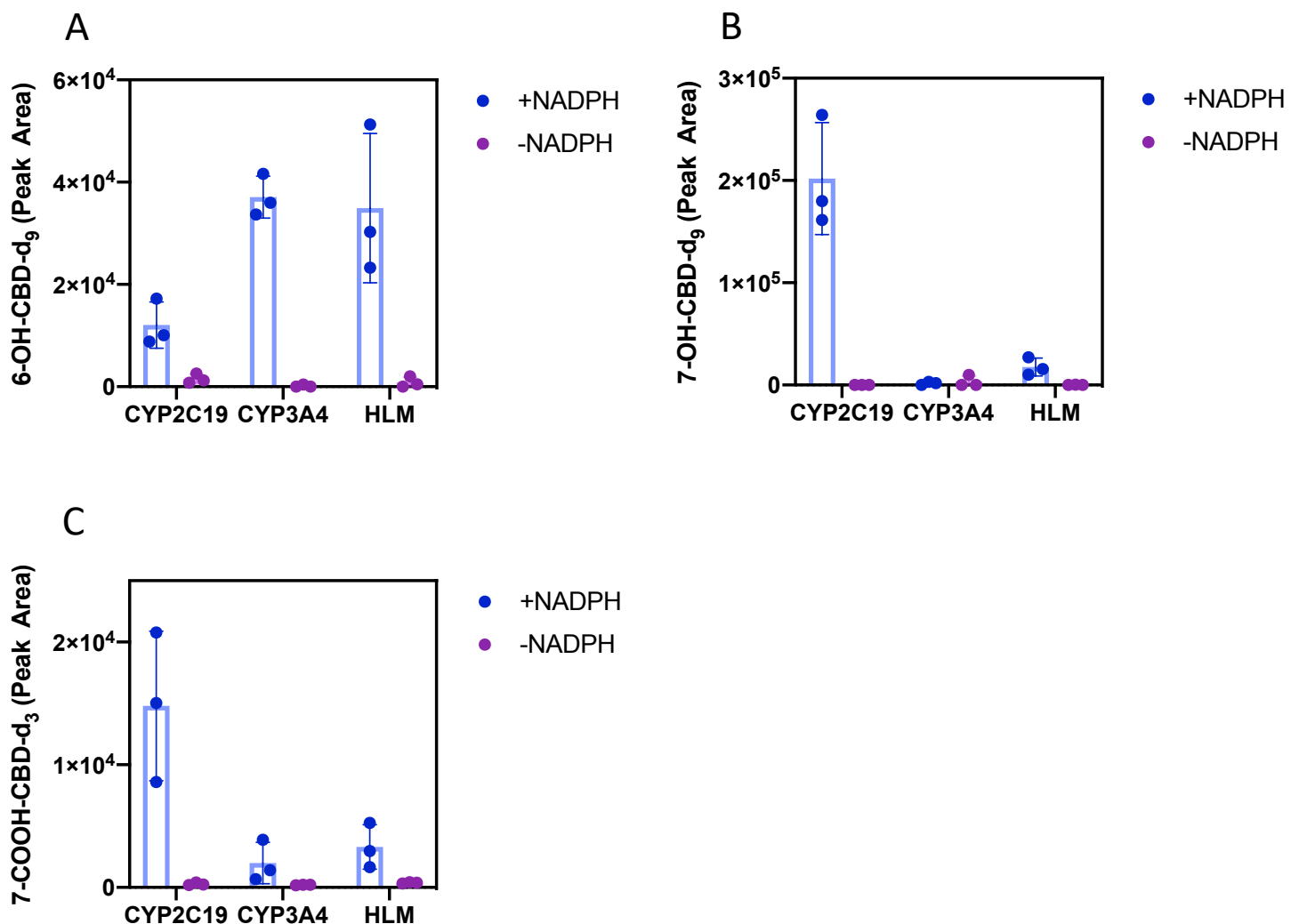


Supplemental Figure S9G. Product ion spectrum of 7-COOH-CBD formed in rCYP3A4 (m/z 343).

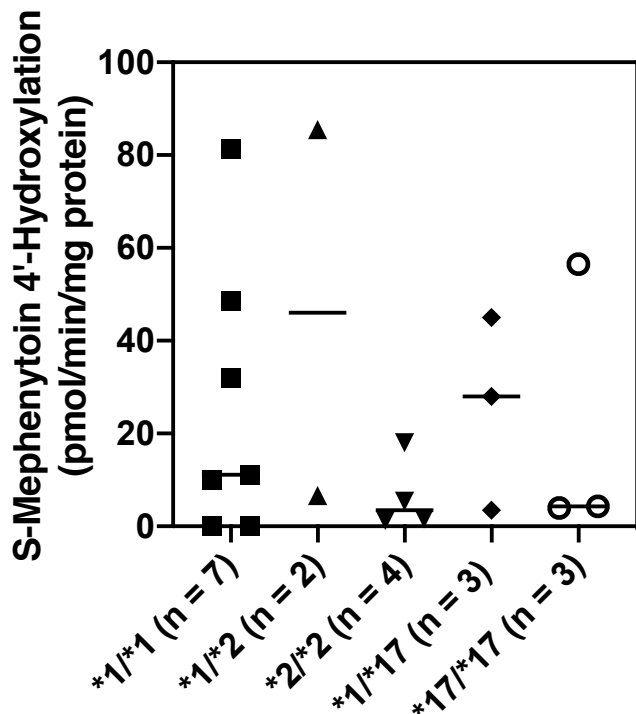
DMD-AR-2020-000350R2



Supplemental Figure S9H. Product ion spectrum of M3 formed in rCYP3A4 (m/z 343).



Supplemental Figure S10. Deuterated cannabinoid metabolite formation by rCYP2C19, rCYP3A4, and HLM. CBD- d_9 (10 μ M) and 7-OH-CBD- d_3 (10 μ M) were incubated with recombinant CYP2C19 (20 pmol/mL), recombinant CYP3A4 (20 pmol/mL) and 150-donor pooled HLM (0.2 mg/mL protein) for 10 min in the presence and absence of NADPH. (A) Formation of 6 α -OH-CBD- d_9 (m/z 338>320), (B) 7-OH-CBD- d_9 (m/z 338>308), and (C) formation of 7-COOH-CBD- d_3 from 7-OH-CBD- d_3 (m/z 346>302) was measured by LC-MS/MS, and results are reported as a peak area. Bars represent the mean \pm SD of three replicates generated in a single experiment.



Supplemental Figure S11. CYP2C19 activity, as measured by S-mephenytoin 4'-hydroxylation, in individual CYP2C19-genotyped HLM. The rate of 4'-hydroxymephenytoin formation was measured as described previously (Murray et al., 2020). Briefly, S-mephenytoin (60 μ M) was incubated with CYP2C19-genotyped human liver microsomes (0.2 mg protein/ml) for 40 minutes. Formation of 4'-hydroxymephenytoin was quantified by LC-MS/MS using a standard curve with known concentrations of 4'-hydroxymephenytoin. The rate of 4'-hydroxymephenytoin formation was compared by CYP2C19 genotype. Bars represent the average metabolite formation for each CYP2C19 genotype. Each point represents the average metabolite formation for each donor determined from a single experiment performed in triplicate.

Reference.

Murray JL, Mercer SL, and Jackson KD (2020) Impact of Cytochrome P450 Variation on Meperidine N-Demethylation to the Neurotoxic Metabolite Normeperidine. *Xenobiotica* 50:132-145.